energies

MDPI

Article

Experimental Investigation of the Impact of CO_2 Injection Strategies on Rock Wettability Alteration for CCS Applications

Stella I. Eyitayo [1,*], Gamadi Talal [1], Oladoyin Kolawole [2], Chinedu J. Okere [1], Ion Ispas [1], Nachiket Arbad [1], Hossein Emadibaladehi [1] and Marshall C. Watson [1]

[1] Bob L. Herd Department of Petroleum Engineering, Texas Tech University, 807 Boston Avenue, Lubbock, TX 79409, USA; narbad@ttu.edu (N.A.); h.emadibaladehi@ttu.edu (H.E.)
[2] John A. Reif, Jr. Department of Civil and Environmental Engineering, New Jersey Institute of Technology, Newark, NJ 07102, USA; oladoyin.kolawole@njit.edu
* Correspondence: stella.eyitayo@ttu.edu

Abstract: Carbon capture and storage (CCS) has been recognized as a pivotal technology for mitigating climate change by reducing CO_2 emissions. Storing CO_2 in deep saline aquifers requires preserving the water-wet nature of the formation throughout the storage period, which is crucial for maintaining rock integrity and storage efficiency. However, the wettability of formations can change upon exposure to supercritical CO_2 ($scCO_2$), potentially compromising storage efficiency. Despite extensive studies on various factors influencing wettability alteration, a significant research gap remains in understanding the effects of different CO_2 injection strategies on wettability in deep saline formations (DSFs). This study addresses this gap by investigating how three distinct CO_2 injection strategies—continuous $scCO_2$ injection (CCI), water alternating with $scCO_2$ injection (WAG), and simultaneous water and $scCO_2$ injection (SAI)—affect the wettability of gray Berea sandstone and Indiana limestone, both selected for their homogeneous properties relevant to CCS. Using a standardized sessile drop contact angle method before and after CO_2 injection, along with core flooding to model the injection process at an injection pressure of 1500 psi and temperature of 100 °F with a confining pressure of 2500 psi, the results indicate a shift in wettability towards more CO_2-wet conditions for both rock types under all strategies with changes in CA of 61.6–83.4° and 77.6–87.9° and 81.5–124.2° and 94.6–128.0° for sandstone and limestone, respectively. However, the degree of change varies depending on the injection strategy: sandstone exhibits a pronounced response to the CCI strategy, with up to a 77% increase in contact angle (CA), particularly after extended exposure. At the same time, WAG shows the least change, suggesting that water introduction slows surface modification. For limestone, the changes in CA ranged from 9% to 49% across strategies, with WAG and SAI being more effective in altering its wettability. This study underscores the importance of selecting suitable CO_2 injection strategies based on rock type and wettability characteristics to maximize carbon storage efficiency. The findings offer valuable insights into the complex interactions of fluid–rock systems and a guide for enhancing the design and implementation of CCS technologies in various geological settings.

Keywords: carbon capture and storage; CO_2 injection strategies; wettability alteration; contact angle; optimizing subsurface storage

check for updates

Citation: Eyitayo, S.I.; Talal, G.; Kolawole, O.; Okere, C.J.; Ispas, I.; Arbad, N.; Emadibaladehi, H.; Watson, M.C. Experimental Investigation of the Impact of CO_2 Injection Strategies on Rock Wettability Alteration for CCS Applications. *Energies* **2024**, *17*, 2600. https://doi.org/10.3390/en17112600

Academic Editors: Bin Pan, Xiaopu Wang, Yujie Yuan, Yujing Du and Naser Golsanami

Received: 13 May 2024
Revised: 24 May 2024
Accepted: 25 May 2024
Published: 28 May 2024

Copyright: © 2024 by the authors. Licensee MDPI, Basel, Switzerland. This article is an open access article distributed under the terms and conditions of the Creative Commons Attribution (CC BY) license (https://creativecommons.org/licenses/by/4.0/).

1. Introduction

Wettability is the capacity of a rock to adhere to one fluid in the presence of another preferentially [1]. This essential property controls the interactions between fluid phases and rock surfaces in porous media, influencing hydrodynamic behavior in subsurface environments. In geological formations such as sandstone and limestone, wettability influences the distribution and movement of fluids like water, oil, and gas, affecting multiphase fluid saturations, relative permeability, and residual saturations [2–4]. A formation's affinity for

water categorizes it as water-wet. Similarly, an affinity for oil or CO_2/gas classifies it as oil-wet or CO_2/gas-wet, respectively. The preferred liquid is termed the wetting phase, with the other the non-wetting phase, affecting the quantity and manner of fluid displacement.

A wetting fluid occupies the thinnest pores due to the attractive forces it exhibits with the formation. It also lines the surface of larger pores—typically quantified as connate water saturation when water is in the wetting phase—and ensures the continuity and flow advantage of the wetting fluid. Conversely, when the fluid is CO_2, it can be residually trapped in smaller pores; however, it flows more easily, increasing its plume migration and area. CO_2's behavior varies depending on the rock surface it interacts with: it acts as a non-wetting phase in strongly hydrophilic, water-wet systems at pressures below 10 MPa and temperatures around 296–298 K, but becomes a wetting phase under supercritical conditions in less or intermediate hydrophilic systems, with the effect intensifying at lower temperatures [5,6]. Supporting this, Plug et al. (2007) observed CO_2 as the wetting phase on clean quartz surfaces at 8.5 MPa and 313 K [7].

Obtaining the contact angle (CA) between the liquid–solid surface, an indication or measure of wettability, can more easily convey the fluid's tendency to spread [8]. Wettability is typically assessed using the Amott–Harvey wettability index (AHM) and sessile drop CA measurement. The AHM involves spontaneous and forced imbibition in initially saturated cores. At the same time, the sessile drop method evaluates the CA directly, proving particularly sensitive to changes in sandstone wettability when exposed to supercritical CO_2 ($scCO_2$) [9]. Wettability, classified via CA measurements into three categories—water-wet, neutrally/intermediate water-wet, and non-water-wet [10] provides crucial insights into fluid behaviors in porous media. CAs are delineated as follows: water-wet (0–75°), neutrally wet (75–120°), and non-water-wet (120–180°). Other authors have classified these as 0–90, 90–120, and 120–180°. Recent developments show a new classification of CA based on water and CO_2. As illustrated by Figure 1, when the CA is less than 70°, the system is water-wet; above 110°, it is CO_2-wet when only water and CO_2 are within the formation. For example, quartz and muscovite mica display strong water-wet properties, with CAs of 0–26° and 0–58°, respectively [11–13]. The formation is termed an intermediate wet system with a CA between 70° and 110°. Another method used in quantifying wettability change is molecular dynamic analytical calculation, which was demonstrated by researchers to give a similar result [14,15]. These types of measurement are referred to as static measurement.

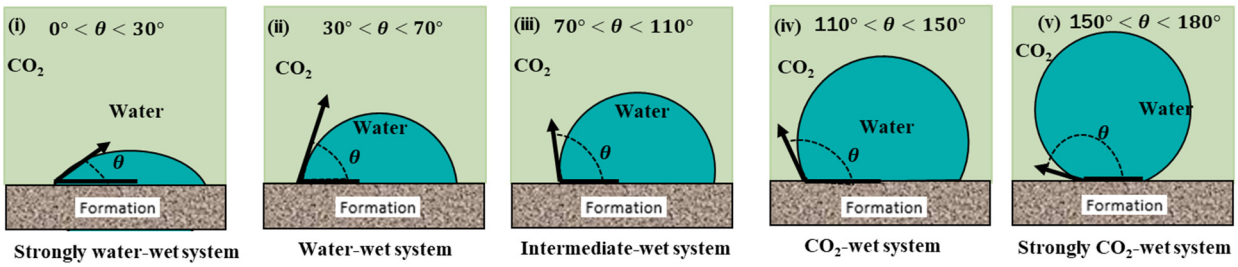


Figure 1. Static contact angle illustration in a CO_2–water–rock system.

1.1. Wettability Alteration

Research has shown that various factors, including the physical properties of the rock, the chemistry of the fluid phases, and the injection conditions, such as pressure and temperature, influence the behavior of CO_2 in subsurface formations. Experimental studies confirm that wettability in geological formations is also influenced by salinity, surface roughness, mineral content, CO_2 density, concentration, and exposure time [16]. Lv et al. (2017) additionally identify interactions between surface contaminants, fluid, pore topology, and capillarity as key factors [17]. In carbonate and some shale formations, wettability alteration is significantly affected by pH, oil composition, fractures, and fissures [9]. The impact of temperature on CA and wettability alteration (WA) shows no consistent trend: CA may increase or decrease with temperature changes, reflecting a transition in water

wettability from strongly to less water-wet or vice versa [15,16,18–20]. Notably, the wettability effect of CO_2 is more pronounced in the subcritical region, indicating a stronger influence at lower temperatures [5]. High-temperature injections can shift wettability from oil-wet to water-wet due to desorption phenomena [21]. An increase in pressure can increase CA, indicating shifts from strongly water-wet to less water-wet or a CO_2-wet system, and this is sustained above 6.7–20 MPa pressure thresholds if other factors remain constant [19,20,22–24]. Jaeger et al. (2010) explained that increasing pressure in CO_2–brine systems might decrease CA, suggesting that CO_2 can become the wetting or non-wetting phase under certain conditions [25]. The impact of ionic strength is better understood than pressure and temperature effects. Higher ionic strength increases WA and significantly changes CA values. Experimental results consistently show that increasing salinity in a CO_2–brine–rock system, primarily composed of quartz or silica, enhances wettability alteration regardless of the measurement method or the type of salt used, whether divalent or monovalent [22,26,27]. However, in the presence of oil, the influence of salinity on CAs is limited. It may either remain unchanged or decrease [28]. Changes in pH can drastically alter wettability; for instance, increasing pH can switch the wettability of mica from water-wet to oil-wet, a dynamic further influenced by CO_2 addition [29,30]. Studies suggest that increasing surface roughness can either increase or decrease CA, with significant implications for mineral dissolution or precipitation-altering surface properties [4,31–33]; hence, it is essential to polish the surface of the formation to be used in the experiment. The type of formation—such as shale, sandstone, limestone, and dolomite—plays a crucial role in how wettability is affected by CO_2 exposure [11,34]. Each mineral responds differently, influencing the optimal selection of caprock properties for CO_2 storage [16,35]. Changes in CO_2 density can modify CA, with denser CO_2 phases generally promoting a shift toward less water-wet conditions [17]. Extended exposure to CO_2 can lead to dynamic changes in CA, demonstrating the importance of time in assessing wettability outcomes [36,37]. Kim et al. (2012) and Al-yaseri et al. (2015) noted that changes within the reservoir could enhance or reduce trapping capacities [18,38]. Wettability alteration mechanisms, such as interfacial tension reduction, mineral dissolution, adsorption, and type of CO_2, play critical roles in these processes. For example, Hirasaki et al. (2011) demonstrated that these mechanisms led to wettability alteration in Berea sandstone when exposed to $scCO_2$ [39]. Dynamic changes in wettability are also driven by prolonged CO_2 exposure [13] These factors, with time, lead to WA, which significantly impacts CO_2 storage strategies. This can lead to accelerated CO_2 migration, affecting mobility and altering solubility and residual trapping capacities. Thus, understanding these variations is crucial for optimizing CO_2 geo-storage efficiency and enhancing containment security. Since storage capacity and efficiencies are affected by several factors, the others must be kept constant to study the effect of one over another. For more details, see Supplementary Materials for Tables S1–S4.

1.2. Impact of Wettability Alteration (WA) on CO_2 Storage

Wettability is crucial in carbon capture and storage (CCS) within deep saline formations (DSFs) or aquifers, where controlling fluid flow significantly impacts the efficiency and success of these processes. WA affects capillary pressure, which affects microscopic sweep efficiency. WA can be either beneficial or detrimental to storage capacity and efficiency. For example, changes within the reservoir can enhance residual trapping [38]. Shifting from strongly to weakly water-wet wettability in quartz in storage conditions can reduce structural and residual trapping capacities [18,40]. Conversely, alterations within the caprock reduce its sealing capacity [41,42].

Various mechanisms responsible for wettability alteration have been identified, including interfacial tension reduction, mineral dissolution, and adsorption. For instance, a study by Hirasaki et al. (2011) found that reduced interfacial tension between CO_2 and water led to rock wettability alteration [39]. Additionally, the study found that mineral dissolution played a role in wettability alteration. In carbonates, Sagbana et al. (2022) stated that the mechanisms responsible for WA are multicomponent ion exchange, electric double-layer

expansion, and dissolution [9]. Investigations such as those by Juanes et al. (2006) have delved into the multiphase flow dynamics of CO_2 in porous media, emphasizing the importance of understanding capillary and viscous forces to predict CO_2 plume behavior and trapping mechanisms effectively [43]. Exposure of rock formations to supercritical CO_2 ($scCO_2$) can change their native wettability, impacting the fluid dynamics and trapping mechanisms crucial for effective CO_2 storage. This alteration can either enhance or reduce the capillary forces, thus altering the saturation functions and affecting storage efficiency and security over time. For instance, a study by Wang et al. (2019) found that exposing sandstone to $scCO_2$ shifted its wettability from water-wet to intermediate-wet, with mineral dissolution playing a significant role in this change [44]. Moreover, Li et al. (2005, 2006) and Chiquet et al. (2005, 2007) demonstrated that CO_2 can diminish the capillary-sealing efficiency of shale and evaporite caprocks by reducing CO_2 breakthrough pressures, thereby limiting storage volumes [30,35,45,46]. While various factors influencing these changes have been studied, the impact of injection strategies and exposure time on wettability alteration reduction has yet to be fully explored and studied.

1.3. Injection Strategy as a Means of Reducing WA

Usually, the traditional approach of CO_2 storage involves continuous CO_2 injection (CCI) into the formation using different phases such as gas or liquid. Recently, $scCO_2$ has been found to be more efficient due to its higher density (0.45–0.7 g/cm^3) compared to the gaseous state (0.002 g/cm^3) or liquid state (0.771 g/cm^3) and better stability than in the liquid state [47,48]. In most cases, the $scCO_2$ is injected continuously into the formation until abandonment. The injection of CO_2 or $scCO_2$ into porous media has been extensively studied over recent decades, primarily focusing on improving oil recovery in enhanced oil recovery (EOR), with less attention paid to improving CO_2 storage [49–54]. One such challenge is the excessive production of CO_2 injected alongside the oil. Azzolina et al. (2015) reported that 23.1–61.8% of CO_2 is retained/stored, with an incremental recovery of 5.3–21.5% [55]. Farajzadeh et al. (2020) indicated that 6–56% of the CO_2 is stored, meaning that 0.43–0.94 kg of CO_2/kg of CO_2 stored will be re-emitted, leading to a CO_2 cycle breakthrough that complicates optimization and makes storing large amounts of CO_2 difficult and potentially unsustainable [56]. Regarding life cycle assessment, more energy is consumed to store up to 56% of CO_2 than is generated from the extra oil produced. Water-alternating gas (WAG) has also been exploited for the same purpose in EOR [57–61]; however, this injection strategy has not yet been applied or studied extensively in geological CO_2 storage in DSFs.

While the injection of CO_2 and its interactions with reservoir rocks are well documented, the specific effects of different injection strategies on wettability—a key factor in determining the sweep efficiency of CO_2 storage in deep saline formations (DSFs)—remain less understood. Wettability significantly influences the distribution and movement of fluids within the rock matrix, thereby affecting the ultimate storage capacity of a reservoir. Comprehensive, systematic studies that isolate the effects of varied CO_2 and brine injection strategies on wettability changes are lacking, especially detailed comparative analyses across different rock types under the same experimental conditions to outline each injection method's effects.

The objectives of this research are twofold: to quantitatively assess wettability changes for different injection strategies—continuous $scCO_2$ injection, brine alternating with $scCO_2$ injection, and simultaneous brine and CO_2 injection—and to evaluate how these strategies affect the wettability of two common subsurface rock types, sandstone, and limestone. This assessment will help determine which $scCO_2$ injection strategy least modifies wettability in a way that could enhance the storage and trapping of $scCO_2$, thereby improving overall subsurface carbon storage efficiency. This study aims to contribute valuable insights into the wettability behavior of rock samples when exposed to $scCO_2$ using different injection strategies, offering data-driven recommendations to enhance carbon storage strategies in DSFs.

2. Materials and Methods

The materials utilized in this experiment include core samples (sandstone and limestone), $scCO_2$, and water, which are discussed in detail below.

2.1. Description of Sample and Preparation

The rock samples chosen for this study were Berea sandstone and Indiana limestone, both widely recognized in geoscientific research for their homogeneity and predictable physical properties. Berea sandstone is noted for its high porosity and permeability, consisting predominantly of quartz grains cemented by silica, making it ideal for fluid injection studies. Indiana limestone, characterized by its calcite composition, provides insights into chemical interactions between CO_2 and carbonate minerals.

Each rock type was prepared into cylindrical core samples approximately 1.5 inches in diameter and 3 inches in length. Before testing, all samples were oven-dried and vacuum-saturated with brine to ensure uniform starting conditions. The wettability measurement method—conventional techniques versus micro-CT—can significantly influence observed effects due to differences in surface interaction and cleaning procedures. Therefore, surfaces were cleaned to minimize their impact on the CA measurement.

Sandstone and limestone, prevalent in CCS and EOR projects, offer distinct physical and chemical characteristics crucial for studying CO_2 injection impacts on wettability. Sandstone, primarily siliciclastic, displays varying porosity and permeability, affecting fluid flow and trapping mechanisms. Limestone, mainly composed of calcite, undergoes chemical reactions with CO_2, potentially altering pore structures and surface properties. Understanding how CO_2 and brine injection strategies modify the wettability of these rocks is key to optimizing CCS techniques across different geological settings.

For the study, the observed average effective porosity for nine gray Berea sandstone core samples ranged from 19.3% to 20.2% and for nine Indiana limestone samples from 19.0% to 21.5%. The observed average absolute permeability was between 28.3 and 138.5 mD for Berea sandstone and 20.8 to 188.5 mD for Indiana limestone. The cores were dried in an oven at 100 °F for 24 h and continuously weighed until a consistent dry weight was achieved, and their porosity and permeability were measured. Before experimentation, the cores were saturated in a vacuum saturator to remove air from the pore spaces, simulating reservoir conditions. This process was maintained for 24 h. Cleaned, polished, and saturated core disks were then subjected to $scCO_2$ saturation using core flooding equipment at a confining pressure of 2500 psi and an injection pressure of 1500 psi at 100 °F. Pretest measurements were taken following this preparation.

Wettability changes were quantified using the CA measurement technique. CAs were determined before and after the injection experiments using a high-resolution camera and image analysis software. The CA at which a liquid–vapor interface meets a solid surface indicates the rock's wettability. A decrease in CA suggests a shift toward more water-wet conditions, while an increase indicates a shift toward oil-wet conditions. This detailed methodology ensures a comprehensive assessment of how different CO_2 injection strategies affect the wettability of sandstone and limestone, providing a robust basis for understanding the implications of these methods on subsurface carbon storage. These experiments comprised three phases: (1) pretest CA measurement using the drop shape analyzer, (2) sample exposure through a core flooding experimental setup, and (3) post-test CA measurement for the two samples of gray Berea sandstone and Indiana limestone at various exposure times.

2.2. Pretest and Post-Test Experimental Setup

The initial CA, formed between the solid surface and the tangent at the droplet contact point, was quantified before exposure to any treatment to determine the surfaces' baseline wetting properties.

In this experiment, the sessile drop technique was employed to measure CAs, utilizing a Drop Shape Analyzer DSA25, as depicted in Figure 2. This technique carefully places a

liquid droplet on a solid surface and measures the angle formed at the liquid–solid–gas interface. The droplet's contour is mathematically modeled using a general conic section equation. Calculating the derivative at the point where the droplet contour intersects with the baseline enables the determination of the slope at the three-phase contact point, thus accurately establishing the CA.

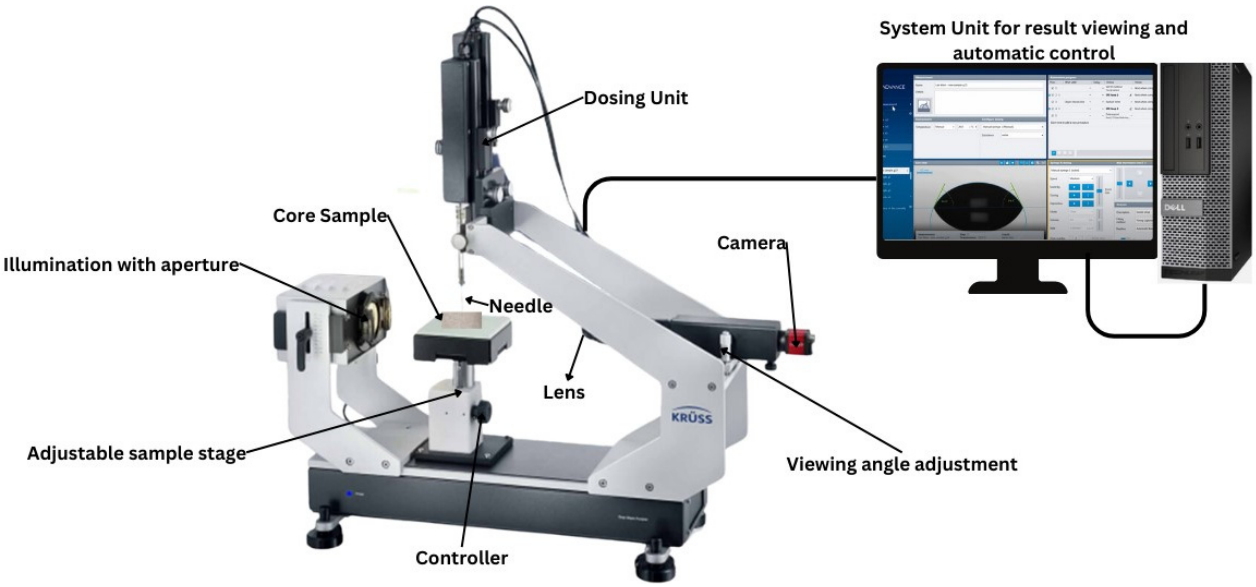


Figure 2. Drop Shape Analyzer (DSA25) for CA measurement showing the needle's and substrate's position.

Unlike some types of CA measurements based on visual observation, these are automatically measured after the diameter of the needle and the surface alignment are properly calibrated. The rock sample is positioned on the adjustable platform, and the drop of liquid is released on the sample. As shown in Figure 2, the DSA25 instrument is crucial for these measurements. It has a high-resolution digital camera and video recording capabilities that capture detailed dynamic changes in droplet behavior and digital processing software. These features allow for continuous monitoring and recording of the drop's shape, providing a robust dataset for analysis. The precise control and advanced imaging capabilities of the DSA25 achieve a measurement resolution of 0.1 degrees, significantly enhancing the accuracy and reliability of the CA measurements.

In this study, the static CA was determined using the ellipse method, which assumes an elliptical shape of the droplet. This method was coupled with large drop weight dynamic dosing to accommodate slightly asymmetrical droplet contours under ambient conditions of 72 °F and 14.7 psi. The substrate was cleaned, placed on an adjustable sample stage, and calibrated to ensure that measurements were taken on a level horizontal plane or the contact baseline. Distilled water was utilized for dosing and introduced slowly onto the substrate surface to facilitate detailed shape analysis and corresponding CA measurement. A lower CA indicates a stronger tendency of the aqueous phase to wet the substrate. The measurements were checked for repeatability at least three times in each experiment.

Sample preparation was standardized across all experiments—samples were cleaned and dried. The pretests and post-tests were conducted before and after subjecting rock samples to various injection strategies. Initial angle measurements were taken using air–water–rock and $scCO_2$–water–rock systems, with post-exposure measurements to inject fluids like $scCO_2$ and water. The final angle measurements were conducted similarly but were limited to the $scCO_2$–water–rock system. The sessile drop method, involving water droplets on an $scCO_2$-immersed substrate, was employed for these measurements.

2.3. Core Flooding Experimental Setup and Conditions

The temperature and pressure conditions selected for these experiments were based on representative subsurface conditions at which $scCO_2$ begins to exist. CO_2 becomes supercritical at a temperature of 304.2 K (89 °F) and a pressure of 73 atm (1072.8 psi), as shown in Figure 3. Its volume has decreased by 0.3% compared to the volume at standard pressure and temperature conditions [48,62,63]. In this phase, CO_2 exists as a single, uniform phase where the density of CO_2 vapor is the same as that of the liquid, thereby eliminating any interface between the two phases. The experimental temperature and pressure must be higher than these values to maintain these phases. The thermodynamic conditions of 1500 psi injection pressure and 100 °F temperature were chosen to simulate $scCO_2$ conditions commonly desired for CO_2 storage in saline formations. These conditions are critical to replicate in order to understand the behavior of CO_2 in realistic storage scenarios.

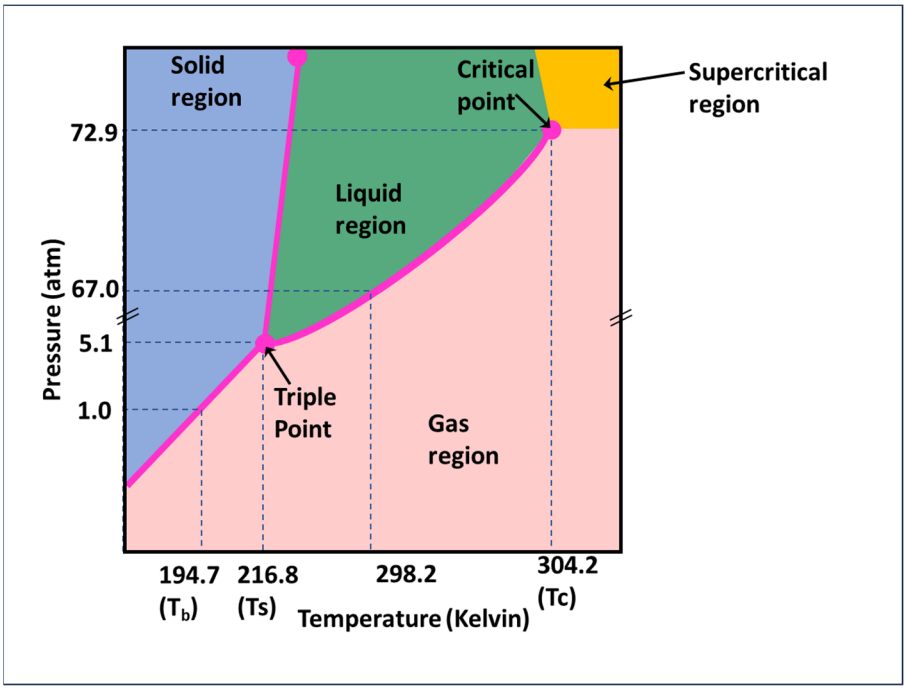


Figure 3. Phase diagram for CO_2 (modified after Atkin and de Paula (2006)).

The experimental setup was designed to investigate various injection strategies involving $scCO_2$ and brine by replicating subsurface geological formation storage conditions. This setup is illustrated in Figure 4.

The setup includes a thermostat capable of regulating temperature from 0–335 °F to ensure desired temperature control (i.e., 100 °F) in the cylinder containing $scCO_2$ throughout the experiments. The gas cylinder is wrapped with a heating jacket to increase the temperature, thus raising the pressure of the gaseous CO_2 to achieve $scCO_2$ formation conditions. It is connected to a corrosion-resistant pressure gauge to monitor system pressures accurately. Additionally, this pressure is used to control the injection pressure to the desired value (1500 psi). Once a pressure of 1500 psi is achieved in the cylinder, $scCO_2$ flows through a CODA Alicat flow meter at a predetermined rate. This flow meter accurately measures injection rates and volumes, enabling precise control over experimental parameters. Pressure transducers, with a maximum pressure rating of 4500 psi, are strategically positioned to measure both inlet and outlet pressures, ensuring that the system operates within the desired pressure ranges (1100–1500 psi). Check valves are also installed in the inlet $scCO_2$ and water flow lines to ensure the unidirectional flow of fluid, which is crucial for maintaining experimental integrity and preventing any backflow.

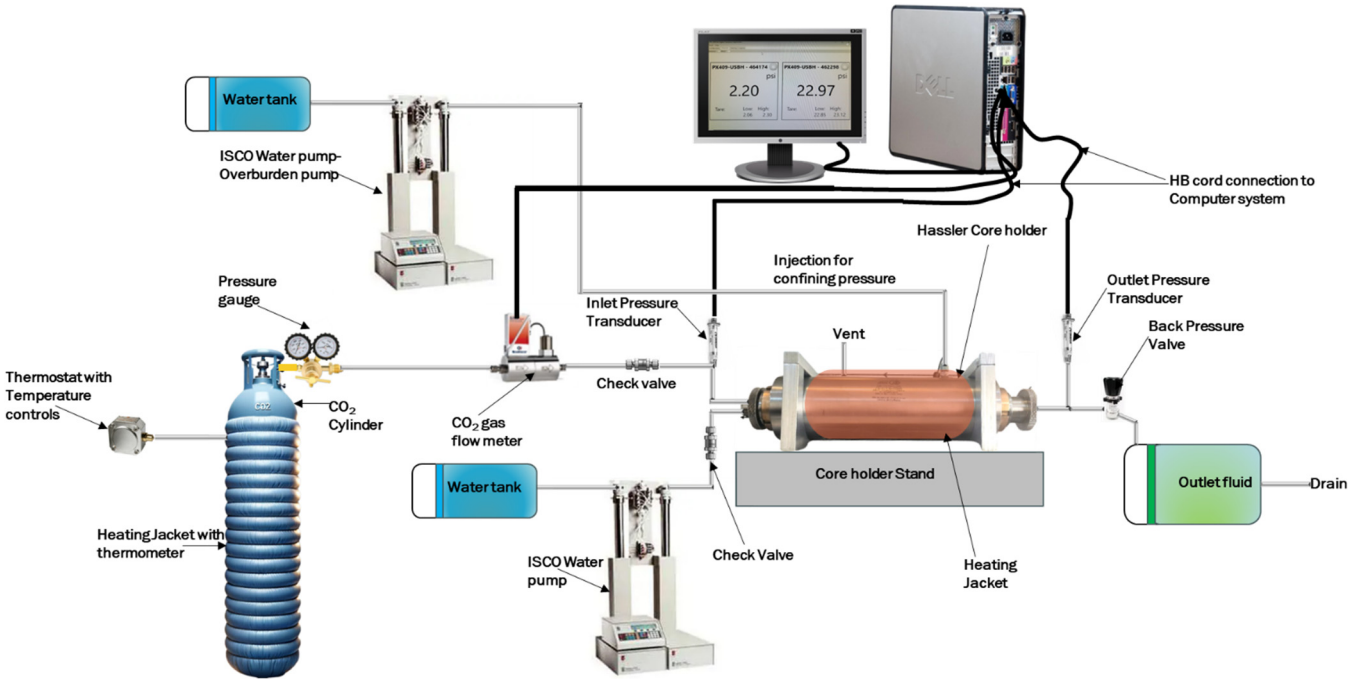


Figure 4. Core flooding experimental setup to simulate different injection strategies for specified exposure time.

The core holder, a critical setup component, is a Hassler Core holder wrapped with a Briskheat composite heating jacket. This configuration serves two primary purposes: preventing heat loss and maintaining the supercritical condition. It also facilitates the flow of fluids through the rock samples under investigation.

A Tescom Back pressure regulator, with an inlet pressure capacity of up to 12,000 psi, is employed to maintain a constant flow pressure of 1500 psi within the system and only vents once the pressure is above 1500 psi. This regulator ensures stability and consistency in experimental conditions, essential for accurate data collection and analysis. Additionally, outlets are provided for the venting or draining of $scCO_2$ or brine, which feeds into a collection system for effluent. This system enables the efficient capture and disposal of experimental byproducts, contributing to the overall safety and integrity of the experiments. Two ISCO water pumps are installed: one allows alternating or simultaneous water injection into the core holder during the WAG and simultaneous $scCO_2$–water aquifer injection (SAI) methods, while the second exerts a confining pressure of about 2500 psi in the system, as required by the experimental procedures. Overall, the experimental setup is comprehensively designed to provide a controlled and precise environment for investigating the behavior of $scCO_2$ and brine within geological formations for different injection strategies.

2.4. Experimental Procedure

Sandstone samples were exposed to carbon dioxide using three exposure scenarios (24 h, 72 h, and 168 h) in core flooding equipment, as shown in Figure 4. This range was selected to observe both the immediate and long-term effects of the exposure on the CAs, providing insights into the kinetics of surface interactions. Different exposure times are synonymous with the aging process in EOR; however, in this case, the fluids were in a dynamic condition for these durations for the different injection strategies considered. The samples were exposed to $scCO_2$ in a Hassler core holder at a 1 mL/min flow rate at a temperature of 100 °F and a confining pressure of 2500 psi. When water was introduced, the rate of 1 mL/min was maintained. Three distinct injection strategies were employed during the experiments: CCI, WAG, and SAI. These methods were chosen to evaluate their respective efficacy in modifying surface properties under controlled conditions. The CCI

strategy involves constant exposure to $scCO_2$. The WAG strategy alternates between $scCO_2$ and brine. In contrast, the SAI strategy is the combined injection of $scCO_2$ and water at the same time, potentially mimicking more dynamic environmental conditions to compare the extent of wettability alteration.

2.4.1. Continuous $scCO_2$ Injection

The cylinder was heated to a temperature of 100 °F using a heating jacket, with the temperature monitored by a thermometer to ensure the CO_2 reached supercritical condition. Each core was first fully saturated with brine using a vacuum saturator to ensure complete saturation. The brine-saturated core sample 1S was then loaded into the core holder. A confining pressure of 2500 psi was applied, and $scCO_2$ was injected at a controlled rate of 1 mL/min, at a pressure of 1500 psi, and at a temperature of 100 °F until a steady state was reached. The pressure was maintained throughout the experiment to ensure the CO_2 remained in the supercritical phase, maximizing its interaction with the rock's surface. The core holder was also heated to 100 °F to prevent any phase change of CO_2 from $scCO_2$ to gas during the injection. $scCO_2$ flowed through with the back pressure valve set to 1500 psi. Once the volume of $scCO_2$ injected reached 75 times the pore volume (PV), which took about 24 h, the injection was stopped, the system was depressurized to remove the core sample immediately, and the post-injection measurement was taken. This is repeated for samples 4S and 7S, except that the injection duration lasted 72 h (225 PV) and 168 h (525 PV), respectively. The same procedure was used for 1L, 4L, and 7L limestone samples.

2.4.2. Alternate $scCO_2$–Water Injection (WAG)

This experiment was like that above: for every 10-pore volume $scCO_2$, 10 PV water is injected without changing experimental conditions. This ensures considerable contact time and that the hydrodynamic drag force will not displace sediments in the cores. This cycle was repeated three times to examine alternating fluids' impact on the rock surfaces' wettability. For comparative analysis of the different injection strategies, the volume of injected $scCO_2$ was limited to 75 PV, 225 PV, and 525 PV for the 24 h, 72 h, and 168 h injections while excluding the time required to inject an equal amount of water. This was repeated for the second and third 24 h of $scCO_2$ injection to 15 PV $scCO_2$ injections.

2.4.3. Simultaneous $scCO_2$–Water Aquifer Injection (SAI)

Similar samples in terms of permeability and porosity were used for the experiment, ensuring a consistent basis for comparing the CCI, WAG, and SAI methods. Initial conditions were carefully established to mirror those in previous tests. Injection rates and pressure were maintained at 0.5 mL/min and 1500 psi, respectively, with water and $scCO_2$ injected at equal volumetric rates. This approach was adopted based on research suggesting that optimized displacement efficiencies are achieved with a balanced injection [64–68]. This could enhance the interface dynamics between the fluids and the rock, potentially improving oil displacement efficiency. The total fluid injection rate was set at 1 mL/min, maintaining the same overall flow rate as in other methods, but allowing for immediate interaction between the brine, $scCO_2$, and rock. The injection duration was aligned with the volumetric benchmarks set in the CCI and WAG experiments, targeting 75 PV, 225 PV, and 525 PV of $scCO_2$ injected at respective experimental durations of 24, 72, and 168 h. The procedure was applied to sandstone samples (3S, 6S, 9S) and limestone samples (3L, 6L, and 9L). Key parameters such as pressure changes, fluid saturations, and recovery rates were monitored throughout the injection process. Pressure sensors and data acquisition systems were deployed to capture a comprehensive dataset, facilitating real-time monitoring and necessary adjustments. After the injections were completed, the CA post-test was conducted.

3. Results

Berea sandstone and Indiana limestone exhibit varying CA influenced by surface treatments, different injection strategies, testing fluids, and exposure durations. Measurements across the Berea sandstone samples' pretest varied from a minimum of 61.3° to a maximum of 83.4°, with a mean initial CA of approximately 72.69°. This variation provided a comprehensive baseline for assessing the impact of subsequent exposure treatments. The initial CA across the samples exhibited relatively low variability, evidenced by a standard deviation of ±5.43, as shown in Table 1. This consistency in initial CAs shows the uniformity in the surface conditions before the injection of $scCO_2$ or water. Such a narrow range in initial measurements is crucial for ensuring that observed differences in post-treatment outcomes are attributable to the core flooding experimental conditions rather than inherent disparities in the sample surfaces. Based on the CA's range of value measurement, Berea sandstone wettability suggests a weak water-wet and intermediate-wet system (Figure 1). Many studies have reported on the CAs of Berea sandstone and Indiana limestone, highlighting variations under different conditions. Donaldson et al. (1969) reported Berea sandstone CAs from 0 to 75° in oil–water–rock systems [69]. Teklu et al. (2015) found Berea sandstone CAs at 20.4° in synthetic salt water and between 21 and 33.3° in carbonates [70]. Zhang et al. (2020) documented high water-wetness for Berea sandstone with angles between 10° and 21°, noting a reduction in equilibrium CA with increased pressure or temperature [41]. Haeri et al. (2022) demonstrated that Berea sandstone CAs range from 15 to 38° when exposed to various CO_2 phases [71]. Mutailipu et al. (2019) observed Berea sandstone CAs between 18.8° and 66.4° under different CO_2 states, investigating wettability alterations under elevated conditions and using the sitting-drop method [24]. These measurements align with the measured value of CAs in this work, except for one sample used.

Table 1. Sandstone CA measurement pretest and post-test.

Sandstone	Pretest CA Mean ± STD (°)			Post-Test CA Mean ± STD (°)		
1S	74.5 ± 4.7	74.1 ± 5.5	74.9 ± 3.9	99.6 ± 2.2	99.5 ± 2.3	99.6 ± 2.5
2S	68.2 ± 4.0	66.5 ± 4.1	69.9 ± 4.3	82.9 ± 3.1	81.5 ± 4.4	84.4 ± 3.1
3S	71.6 ± 3.1	70.4 ± 3.2	72.9 ± 3.0	86.1 ± 0.5	85.2 ± 0.8	86.9 ± 0.4
4S	62.3 ± 3.1	63.0 ± 2.9	61.6 ± 4.4	106.5 ± 2.8	105.9 ± 3.0	107.2 ± 3.9
5S	73.7 ± 2.9	73.7 ± 2.7	73.7 ± 3.1	90.9 ± 2.3	91.6 ± 2.9	91.6 ± 2.9
6S	75.4 ± 1.4	77.2 ± 1.6	73.6 ± 1.3	84.3 ± 1.5	85.4 ± 2.5	83.1 ± 1.8
7S	72.65 ± 5.2	70.0 ± 6.3	75.3 ± 5.5	123.3 ± 12.4	124.2 ± 14.4	122.3 ± 11.1
8S	82.4 ± 1.2	81.4 ± 1.9	83.4 ± 1.9	106.1 ± 3.1	104.1 ± 4.8	108.1 ± 2.3
9S	73.5 ± 2.4	74.7 ± 2.5	72.4 ± 2.4	103.0 ± 2.1	103.3 ± 3.9	102.6 ± 0.9

Figures 5–7 show digital images of the pretest and post-test CA measurements for 168 h of exposure time for the three injection strategies as evidence of how the droplet shape evolved due to its modification by $scCO_2$. The final wettability, assessed after implementing CCI, WAG, and SAI injection strategies, is also shown in Table 1. Post-exposure, the final CA was recorded to assess the changes induced by the interaction with the exposure environment. These angles showed a considerable shift, ranging from 81.5° to 124.2°, suggesting significant surface property changes due to the injection of $scCO_2$ through the samples. The average final CA observed was approximately 98.42°, indicating a general trend towards increased hydrophobicity or alteration of other surface characteristics.

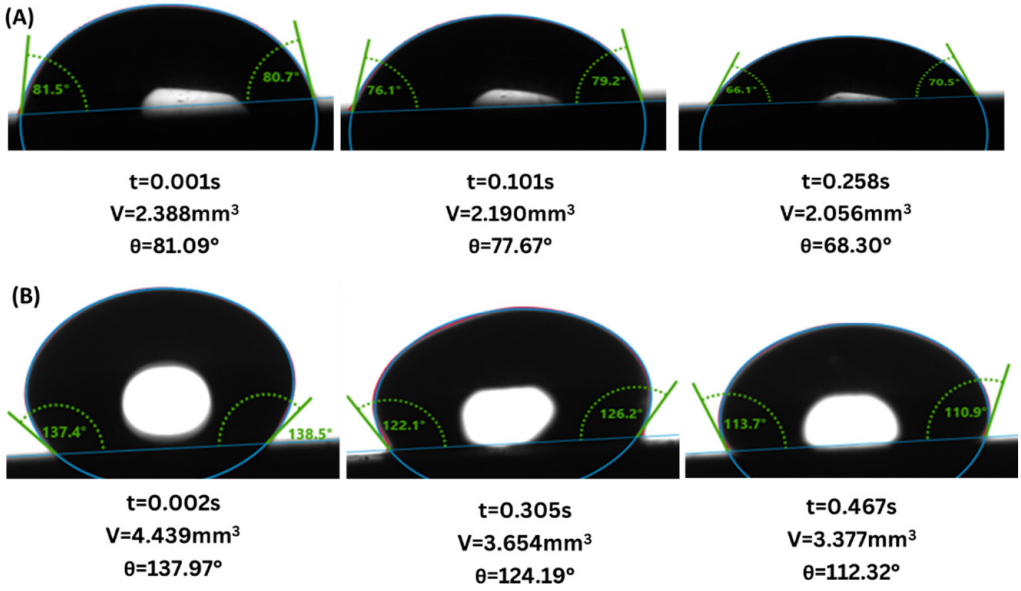


Figure 5. Sequential digital images of the sessile water drop on the $scCO_2$-saturated sandstone substrate sample 7S: (**A**) pretest CA and (**B**) post-test CA after 168 h of CCI of $scCO_2$.

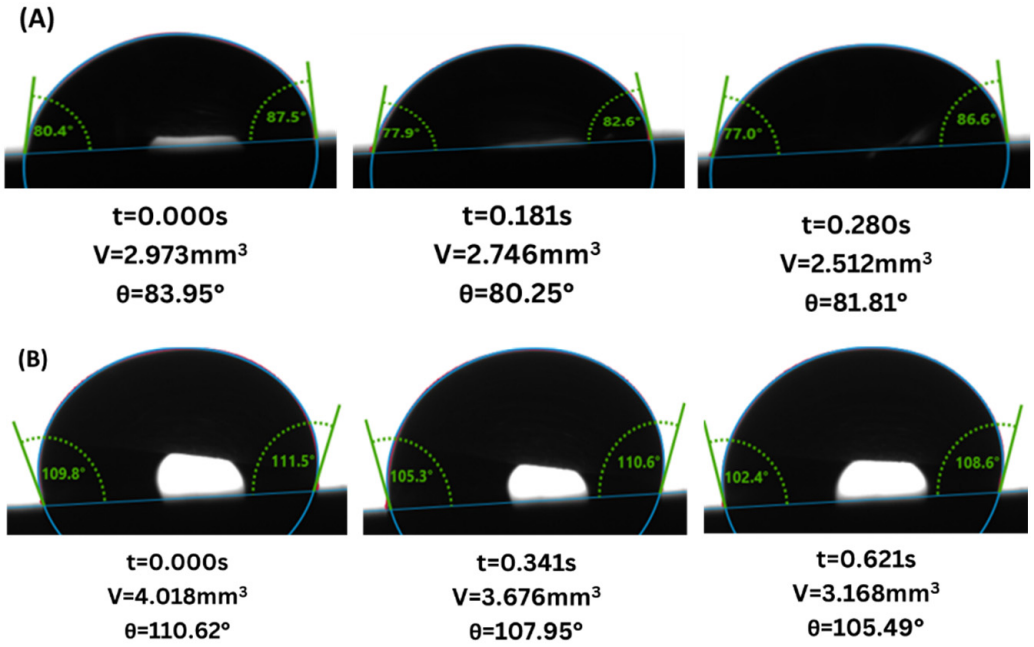


Figure 6. Sequential digital images of the sessile water drop on the $scCO_2$-saturated sandstone substrate sample 8S: (**A**) pretest CA and (**B**) post-test CA after 168 h of WAG of $scCO_2$ and water.

In contrast to the initial CAs, the final CAs demonstrated greater variability, with a standard deviation of about 13.09. This increased spread indicates a diverse range of surface responses to the treatments applied. This can be attributed to the differential impact of the exposure types and the injection strategies employed. The variation in final CAs highlights the influence of experimental conditions on surface properties, providing a rich dataset for analyzing each treatment strategy's effectiveness and potential applications. The CA range suggests that the Berea sandstone changed from a weak water-wet system to a weak CO_2-wet system. This result is corroborated by Mutailipu et al. (2019), where the influence of $scCO_2$ and water at elevated temperatures and pressures led to Berea sandstone samples becoming less water-wet as the CO_2 phase state changed from subcritical to supercritical [24]. The observed changes in CAs suggest modifications in

surface properties, potentially pointing to alterations in surface hydrophobicity or other physical characteristics. For more of these for 24 h and 72 h changes, see the supplementary information (i.e., Figures S1–S6 in Supplementary Materials).

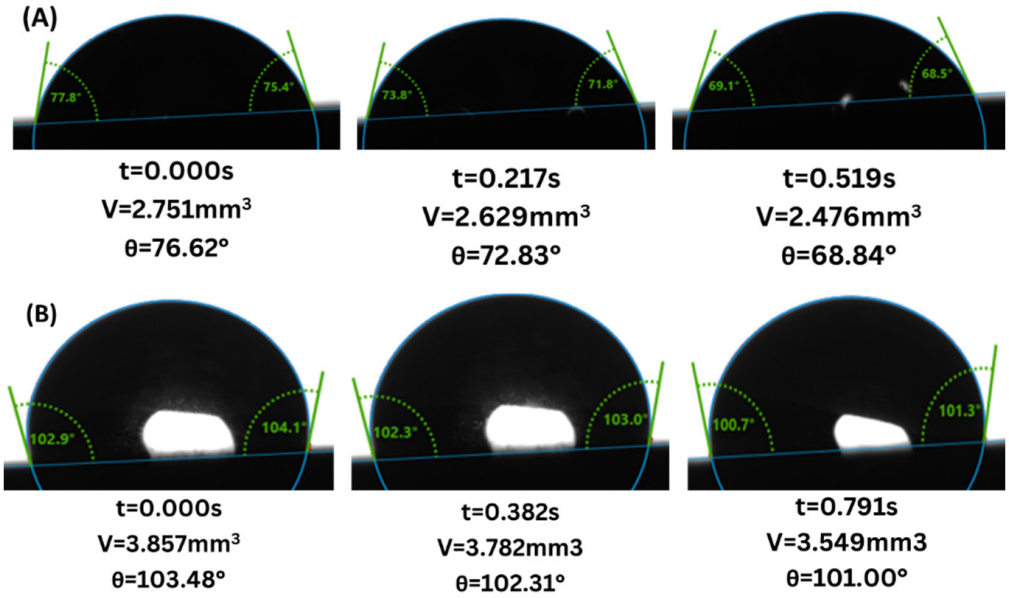


Figure 7. Sequential digital images of the sessile water drop on the $scCO_2$-saturated sandstone substrate sample 9S: (**A**) pretest CA and (**B**) post-test CA after 168 h of SAI of $scCO_2$ and water.

Similarly, Indiana limestone CA ranged from 77.6 to 87.9° with an average of 83.6° with a narrow variability, as indicated by a standard deviation of 2.80°, which is slightly higher than the Berea sandstone, but still indicates a water-wet to intermediate-wet system, as shown in Table 2. Christensen et al. (2017) measured Indiana limestone CAs from 55.1 to 150.0°, which agrees with our results [72].

Table 2. Limestone CA measurement pretest and post-test.

Limestone	Pretest CA Mean ± STD (°)			Post-Test CA Mean ± STD (°)		
1L	86.3 ± 2.9	84.7 ± 2.9	87.9 ± 3.5	100.3 ± 0.9	100.9 ± 0.8	99.6 ± 1.1
2L	85.9 ± 0.5	83.9 ± 0.4	87.9 ± 0.6	96.3 ± 1.6	95.9 ± 1.7	96.6 ± 1.5
3L	84.1 ± 2.0	83.8 ± 1.6	84.5 ± 3.2	95.1 ± 1.2	94.6 ± 1.3	95.5 ± 1.1
4L	83.1 ± 3.4	82.4 ± 3.4	83.7 ± 3.4	116.4 ± 2.6	116.1 ± 2.1	116.7 ± 3
5L	78.5 ± 3.6	79.5 ± 3.3	77.6 ± 4.0	102.8 ± 3.9	102.8 ± 3.9	102.8 ± 3.8
6L	78.4 ± 3.8	78.2 ± 3.4	78.7 ± 4.5	115.2 ± 2.9	115.2 ± 2.7	115.2 ± 3.4
7L	86.6 ± 1.3	86.2 ± 1.3	87.0 ± 1.4	123.1 ± 3.5	122.9 ± 3.9	123.3 ± 3.2
8L	85.5 ± 1.7	85.2 ± 3.4	85.9 ± 2.4	127.8 ± 1.5	127.6 ± 1.5	128.0 ± 1.6
9L	81.3 ± 1.5	80.4 ± 1.6	82.1 ± 2.2	121.0 ± 0.3	120.6 ± 0.3	121.5 ± 0.3

Post-exposure, the CAs shift significantly from 94.6 to 128.0°, representing a CO_2-wet system with lower variability than sandstone samples showing increased variability (standard deviation of 3.5°). The increases in CAs show considerable variability, ranging from modest increases around 10° to significant shifts exceeding 40°. This variability underscores the nuanced response of CAs to the injection processes. Dos Santos Lucas et al. (2020) and Felix Feldmann et al. (2021) measured original and varying CAs in Indiana limestone using distilled and various saline waters, respectively [73,74], highlighting substantial variations dependent on the fluid medium. These studies corroborate the

sensitivity of rock surface wettability to environmental conditions and fluid composition. Figures 8–10 display digital images capturing the evolution of droplet shapes before and after 168 h of exposure, demonstrating the impact of $scCO_2$ on the CA measurements for the three injection strategies. These images visually illustrate how the droplet shape has been altered due to the interaction with $scCO_2$. For more of these for 24 h and 72 h changes, see the supplementary information (i.e., Figures S7–S12 in Supplementary Materials).

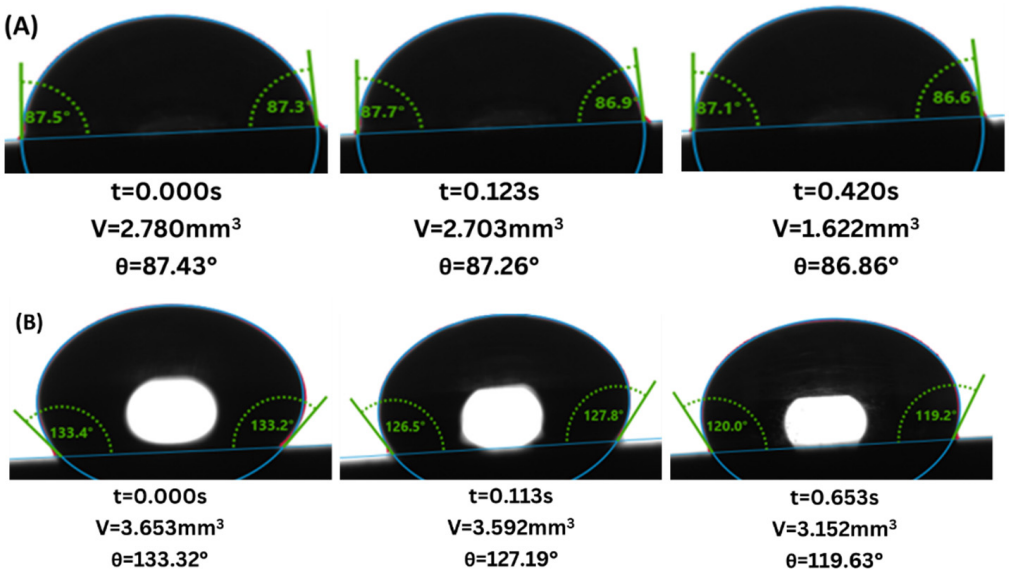


Figure 8. Sequential digital images of the sessile water drop on the $scCO_2$-saturated limestone substrate sample 7L: (**A**) pretest CA and (**B**) post-test CA after 168 h of CCI of $scCO_2$.

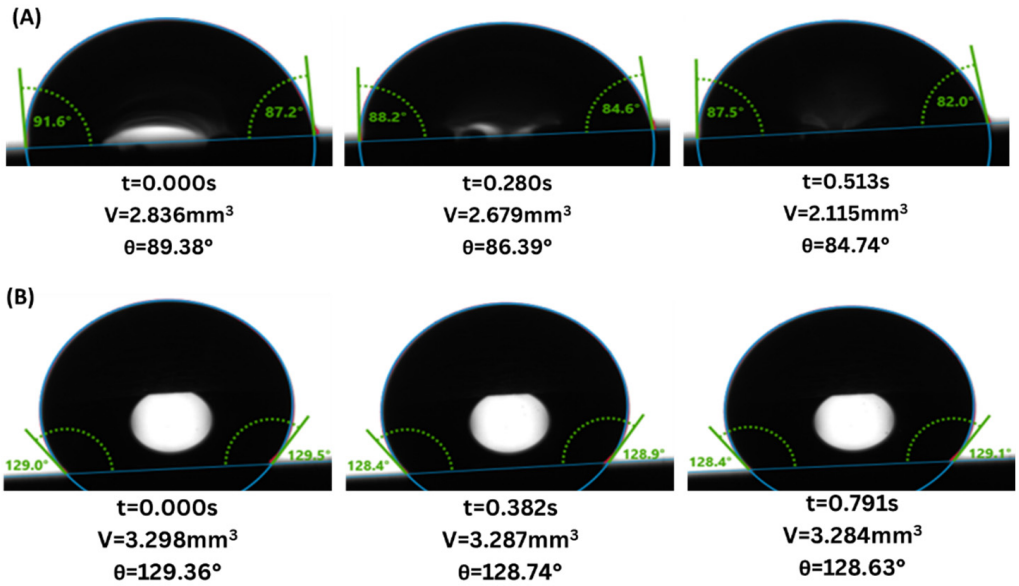


Figure 9. Sequential digital images of the sessile water drop on the $scCO_2$-saturated limestone substrate sample 8L: (**A**) pretest CA and (**B**) post-test CA after 168 h of WAG of $scCO_2$ and water.

For repeatability measurement, at least ten 10 steps and 25 steps of data count were measured for each injection scenario for sandstone and limestone, respectively, as shown in Figure 11, to ensure that the measurement was consistent for some time. In addition, for each sample, the pretest and post-test measurements were taken twice to ensure consistency in the results.

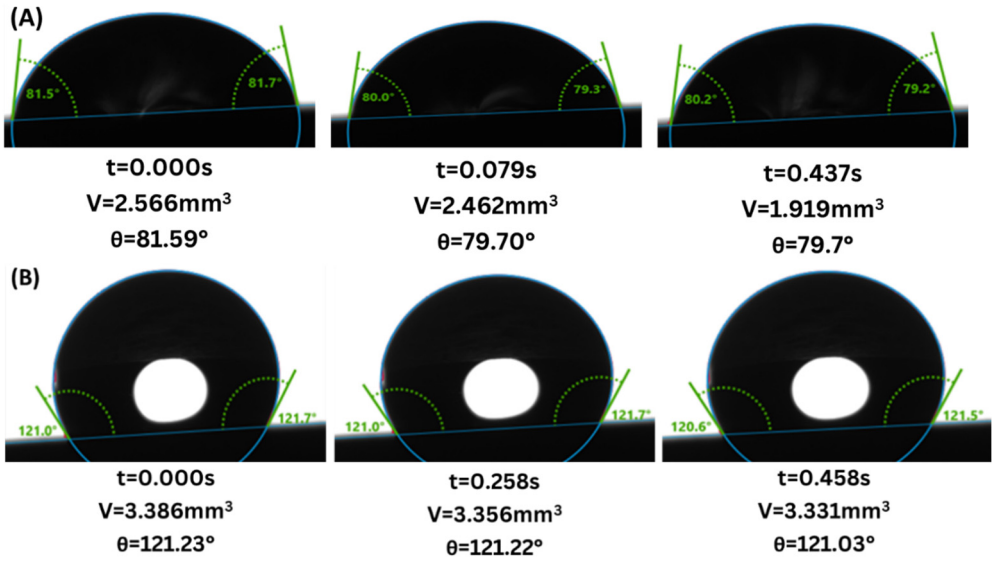


Figure 10. Sequential digital images of the sessile water drop on the $scCO_2$-saturated limestone substrate sample 8L: (**A**) pretest CA and (**B**) post-test CA after 168 h of SAI of $scCO_2$ and water.

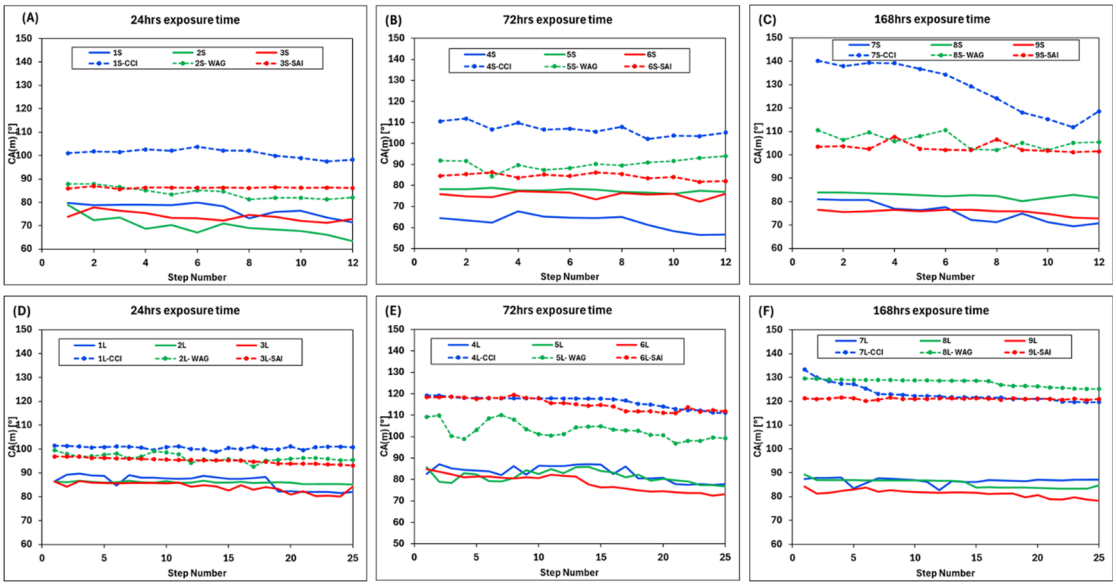


Figure 11. Pretest and post-test CA with the range of steps measurement for (**A**) sandstone exposure for 24 h, (**B**) sandstone exposure for 72 h, (**C**) sandstone exposure for 168 h, (**D**) limestone exposure for 24 h, (**E**) limestone exposure for 72 h, and (**F**) limestone exposure for 168 h.

4. Discussion

Wettability alterations have direct implications for carbon storage efficiency. More water-wet conditions generally enhance the capillary trapping of CO_2, thereby increasing the security and capacity of CO_2 storage. This effect is crucial in preventing CO_2 from migrating upwards and potentially leaking from the reservoir; hence, there is a need to conserve the original wettability of the formation. This is not the case, especially when the formation is exposed to $scCO_2$, because the WA occurs, making the formation CO_2-wet. To reduce this effect, water is introduced in the injection strategy to slow the effect or prevent early and fast surface modification. The results of the wettability experiments indicated different effects for each injection strategy in sandstone and limestone. Variation in exposure times was crucial for assessing the kinetics of surface interactions over both short and extended periods, aiding in understanding the temporal dynamics of surface

modifications, critical for applications in CCS. Figure 12 illustrates that CA increased for sandstone, with longer exposure times correlating with more substantial changes.

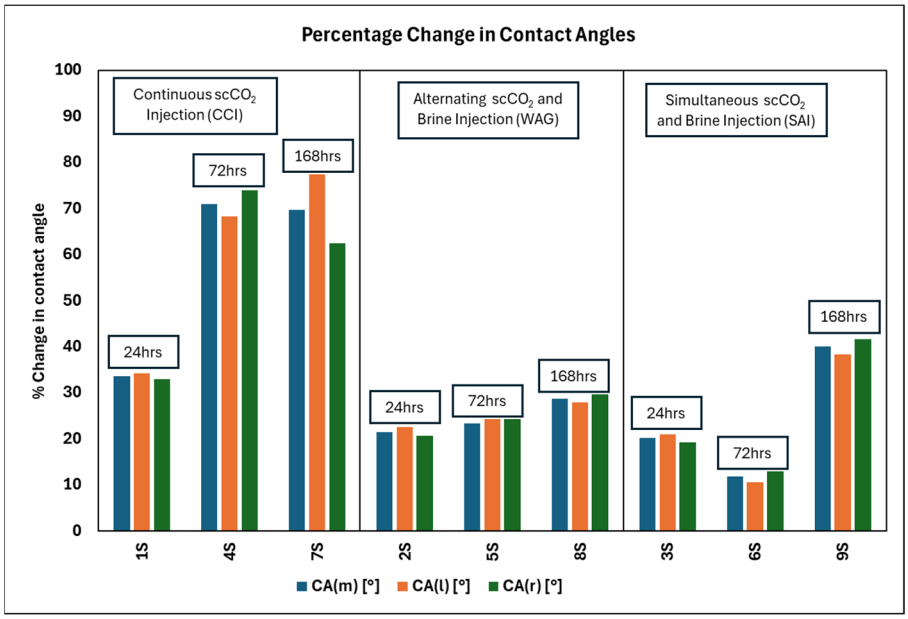


Figure 12. Changes in static CA measurement for each injection strategy at different exposure times in a sandstone formation.

4.1. Gray Berea Sandstone

For the CCI strategy, the initial average CA in sandstone post-injection increased by 32–77% depending on the exposure duration, indicating a significant shift toward more CO_2-wet conditions. Specifically, Berea sandstone's largest variation occurred with a 168 h exposure (525 PV $scCO_2$ injection). This trend suggests that the surface–treatment interaction intensifies over time due to increased absorption, diffusion, or chemical reactions at the surface. At the same time, a steady increase in post-injection increased by 20–29%. This shows that WAG resulted in the least changes, suggesting that the water introduction slows surface modification due to dilution and limited chemical reaction or formation of weak acid. This is not the case in the SAI strategy, because the CA increases slightly (i.e., lower than the WAG increase) in the 24 and 72 h injection time, but was followed by a larger increase in the longer injection period. This may be due to sample 9S having higher permeability than 3S and 6S coupled with a longer injection period. This is because permeability plays a significant role in the fluid–rock interactions that determine the CA, such as uniform fluid distribution and easier flow of fluids. In rocks with higher permeability, $scCO_2$ can more readily penetrate the pore structure, potentially altering the surface properties more extensively than in rocks with lower permeability. Permeability affects capillary pressure, which influences the wetting phase behavior in porous media. Lower permeability typically results in higher capillary pressures, which can enhance the capillary trapping of $scCO_2$ and influence the CA by modifying the wetting characteristics of the rock.

For the Berea sandstone, the data indicate significant variability and differing impacts of $scCO_2$ injection strategies on the CAs of samples, with the only significant difference observed between CCI and SAI. CCI shows a broad range of angle changes, indicating high variability in its impact on the samples, as shown in Figure 12. WAG, in contrast, presents a smaller and more consistent change, suggesting a less aggressive impact. Similarly, SAI demonstrates variability, but less so than CCI. Statistically, to further quantify these observations, the mean changes in CAs for CCI, WAG, and SAI are 39.9° (with a variability of 13.02°), 19.93° (with a variability of 5.07°), and 17.37° (with a variability of 10.85°), respectively, as shown in Figure 13.

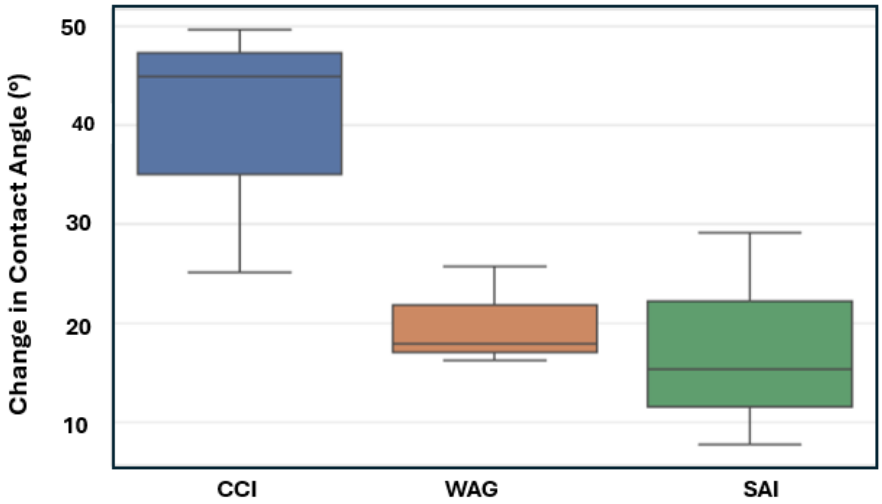


Figure 13. Boxplot showing the variability of change in CA for Berea sandstone.

4.2. Indiana Limestone

For the Indiana limestone, the change in CA varies across the board depending on the exposure time and the injection strategy, as in the case of sandstone. These ranges are similar across all the injection strategies; for instance, the initial average CA post-injection is 13–42%, 9–49%, and 12–49% for CCI, WAG, and SAI strategies, respectively, indicating that CCI is a preferred injection strategy for CO_2 storage in limestone, as shown in Figure 14. For the WAG and SAI strategy, limestone is more responsive to surface modifications when water is introduced. Notably, the most substantial alteration and changes in limestone CA were observed, with CAs increasing from 85.9° to 128.0° under SAI conditions. This suggests that the dynamics and interactions between the injected fluids and rock surfaces vary significantly across different injection methods, leading to marked differences in surface-wetting properties. These findings have significant implications for optimizing fluid injection strategies in geological formations. The average changes in CA due to different injection strategies reveal distinct patterns: WAG results in an average change of 30.50°, CCI has the least change with an average of 11.74°, and SAI leads to the most pronounced change at 39.51° for the limestone samples, as shown in Figure 15.

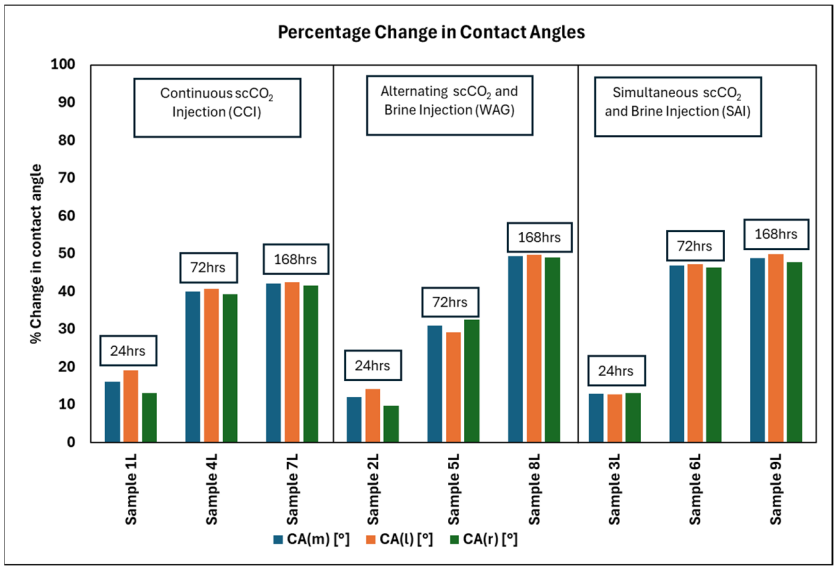


Figure 14. Changes in static CA measurement for each injection strategy at different exposure times in a limestone formation.

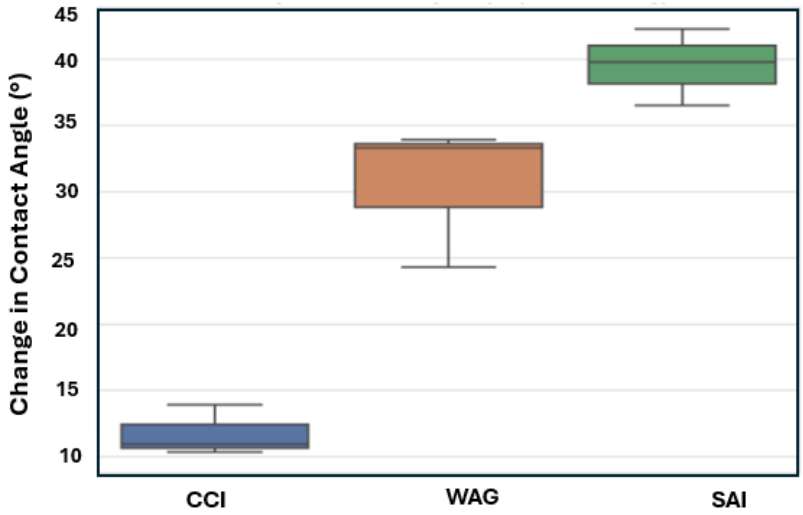


Figure 15. Boxplot showing the variability of change in CA for Indiana limestone.

4.3. Significance of Wettability Alteration in CCS

CCS is a key strategy in the global effort to mitigate greenhouse gas emissions and combat climate change. This method involves capturing CO_2 from industrial and energy-related sources, transporting it to a storage site, and injecting it into underground geological formations to isolate it from the atmosphere. One significant aspect of CCS is the impact of CO_2 on the wettability of the rock formations. Typically, saline aquifers, where water is the native fluid, are inherently water-wet. However, introducing $scCO_2$ can alter this native wettability, significantly changing the fluid dynamics within these formations.

The experimental results demonstrate significant wettability alterations in both sandstone and limestone due to the different CO_2 injection methods. The observed shift towards more CO_2-wet conditions suggests that $scCO_2$ interactions with the rock matrices are conducive to altering the surface energy, thereby influencing fluid retention and migration patterns. This effect is slowed when water is introduced to the system, except for limestone samples, where changes were more dramatic due to its chemical reactivity. The introduction of water with $scCO_2$ can cause mineral dissolution and subsequent reprecipitation. The interactions between $scCO_2$, brine, and rock surfaces significantly affect storage efficiency in geological CO_2 storage. These interactions are primarily governed by the chemical properties of the substances and their interplay under subsurface conditions. $scCO_2$ dissolves or precipitates minerals, notably affecting carbonate rocks like limestone, potentially altering their porosity, permeability, and wettability [75]. This process fundamentally alters the surface characteristics of the rock. These effects are also influenced by the CO_2's partial pressure, temperature, and water presence. When brine is used, it can lead to ion exchange, pH shifts, and changes in rock surface charge, which together can modify fluid–rock interactions and affect $scCO_2$ mobility. In addition, when $scCO_2$ dissolves in brine, it forms carbonic acid, which can react further with rock minerals, altering formation mineralogy and potentially increasing porosity and changing flow paths for CO_2. These chemical interactions can transform rock wettability from water-wet to CO_2-wet, impacting the capillary trapping mechanism essential for CO_2's secure storage. The rate of these interactions is influenced by thermodynamic and kinetic factors, including temperature, pressure, and rock surface area, with higher temperatures generally accelerating the chemical reactions and enhancing their effects. X-ray diffraction (XRD) and scanning electron microscopy with energy-dispersive X-ray spectroscopy (SEM-EDS) are required to ascertain whether the element is dissolved or precipitated, coupled with pH measurement and analyses of ionic concentration. These are beyond the scope of this study and hence are recommended as further analyses in explaining the element or compound responsible for reduced WA when using different injection strategies.

This alteration affects the residual and solubility trapping mechanisms crucial for effective CO_2 storage, influencing critical capillary forces in trapping CO_2 within pore spaces. Wang et al. (2013) showed that a 38% change in CA would lead to a 5−10% difference in capillary trapping or pressure [76]. Such changes can either enhance or diminish the storage capacity and stability of subsurface CO_2 reservoirs. Furthermore, the interaction between CO_2 and reservoir rocks may trigger geochemical reactions, potentially affecting the rock's structural integrity and influencing the feasibility and safety of CCS technologies. Based on these experimental studies, the effect can be slowed when WAG or SAI is used, especially when sandstone is involved.

Understanding how CO_2 gets trapped in porous media is essential for determining target formations' storage capacity and predicting potential CO_2 trapping in aquifers. Changes in wettability due to CO_2 exposure can lead to shifts from water-wet to CO_2-wet conditions, affecting the long-term security of CO_2 storage. The implications of observed wettability changes for the long-term stability of CO_2 storage include potential impacts on capillary trapping and the integrity of the storage site. This is why tailored injection strategies such as WAG or SAI can mitigate these effects, especially in sandstone formations. These strategies help manage the wettability and enhance the effectiveness of carbon storage.

Moreover, the CO_2 wettability of caprock is crucial for ensuring a reservoir's structural trapping and containment security. Under reservoir conditions, caprock wettability changes can significantly reduce sealing efficiency, highlighting the need to adjust reservoir simulation models to reflect these conditions and ensure reliable predictions and operational security. Reducing WA is vital to optimizing CO_2 geo-storage efficiency and security of containment [77]. Overall, these findings provide a deeper understanding of how different injection strategies can be tailored to maximize the efficiency of CO_2 sequestration based on specific rock types. Further research is recommended to explore the long-term stability of the altered wettability conditions and their real-world applicability in large-scale carbon storage projects.

5. Conclusions

This study systematically investigated the impact of three CO_2 injection strategies on the wettability of sandstone and limestone, providing significant insights into the dynamics of fluid–rock interactions under varying strategies. The research emphasized the importance of maintaining more water-wet conditions, as they enhance the capillary trapping of CO_2, thereby increasing the security and capacity of CO_2 storage. This research demonstrates the necessity for further exploration and development of tailored CO_2 injection strategies, which are essential for harnessing their full potential in CCS and alleviating climate change. The main findings include the following.

- Wettability Change: Both sandstone and limestone changed towards more CO_2-wet conditions across all injection strategies due to changes in CA from the range of 61.6–83.4° to 77.6–87.9° and from 81.5–124.2° to 94.6–128.0° for sandstone and limestone respectively. The decreased water-wetness suggests that capillary trapping of CO_2 is limited and crucial for the long-term security and efficacy of geological carbon storage.
- Injection Strategy Efficiency: The results show variability in surface response depending on the injection strategy employed. Sandstone displayed more substantial changes in wettability for CCI, with a 77.4% change in CA. In comparison, WAG was more effective in reducing the WA with the least change of 29.6%, followed by the SAI strategy with a change of 41.7% maximum. Changes in CA and wettability were similar across strategies in limestone, with changes of 42.5%, 49.7%, and 49.9% in CCI, WAG, and SAI methods, highlighting its chemical reactivity with $scCO_2$ and water. This suggests that WAG and SAI may enhance the interaction between CO_2, brine, and rock surfaces, potentially leading to better CO_2 trapping mechanisms in sandstone formations.

- Exposure duration: Across all samples, CA gradually increased as the exposure time increased, except for the SAI process when sample 6S was exposed for 72 h. This is related to the permeability variability of these samples.
- Rock Type Specificity: The results underscored the importance of considering rock type when selecting CO_2 injection strategies, as a rock's chemical composition and physical properties significantly influence the outcome of wettability changes. The differential response between sandstone and limestone to the same injection strategies indicates that tailoring the injection approach based on specific geological settings of a storage site could optimize sequestration results. In this case, the WAG method with a sandstone formation gave the most favorable result for CO_2 storage. This prolongs WA and hence maintains the water-wet nature of formation for longer than CCI.

Future Research

While this study provides foundational insights, further investigation to bridge existing knowledge gaps is required, as follows.

- Study surface morphology of the rock samples before and after injection, providing visual evidence of physical changes at the microstructural level using the SEM. In addition, X-ray diffraction patterns will also show mineralogical changes post-injection, particularly in limestone, supporting the observed wettability results.
- Future studies should focus on the long-term stability of wettability changes and their implications over the lifespan of a CO_2 storage project (for instance, 6 months to 1 year). Understanding how these changes persist under varying geological and operational conditions is crucial.
- Exploring the role of different brine compositions and additives that might enhance wettability changes or react chemically with CO_2 and rock could further optimize injection strategies.
- Developing comprehensive models that integrate fluid dynamics, rock chemistry, and wettability changes would help predict outcomes more accurately and design better injection protocols.

Supplementary Materials: The following supporting information can be downloaded at https://www.mdpi.com/article/10.3390/en17112600/s1. Supplementary S1. Other figures of Contact angle change. Supplementary S2: Contact angle and wettability. References [78–99] are cited in the Supplementary Materials.

Author Contributions: Conceptualization, S.I.E. and M.C.W.; Methodology, S.I.E.; Validation, G.T., O.K., I.I. and H.E.; Formal analysis, S.I.E., O.K. and N.A.; Investigation, S.I.E. and C.J.O.; Resources, M.C.W.; Writing—original draft, S.I.E.; Writing—review & editing, G.T., O.K., I.I., N.A., H.E. and M.C.W.; Supervision, G.T. and M.C.W.; Funding acquisition, M.C.W. All authors have read and agreed to the published version of the manuscript.

Funding: This research received no external funding.

Data Availability Statement: The original contributions presented in the study are included in the article/Supplementary Materials, further inquiries can be directed to the corresponding author.

Conflicts of Interest: The authors declare no conflict of interest.

References

1. Ahmed, T. *Reservoir Engineering Handbook*, 4th ed.; Gulf Professional Publishing: Amsterdam, The Netherlands, 2010. [CrossRef]
2. Iglauer, S.; Al-yaseri, A.Z.; Rezaee, R.; Lebedev, M. CO_2 wettability of caprocks: Implications for structural storage capacity and containment security. *Geophys. Res. Lett.* **2015**, *42*, 9279–9284. [CrossRef]
3. Iglauer, S.; Wülling, W.; Pentland, C.H.; Al-Mansoori, S.K.; Blunt, M.J. Capillary-trapping capacity of sandstones and sandpacks. *SPE J.* **2011**, *16*, 778–783. [CrossRef]
4. Tudek, J.; Crandall, D.; Fuchs, S.; Werth, C.J.; Valocchi, A.J.; Chen, Y.; Goodman, A. In situ contact angle measurements of liquid CO_2, brine, and Mount Simon sandstone core using micro X-ray CT imaging, sessile drop, and Lattice Boltzmann modeling. *J. Pet. Sci. Eng.* **2017**, *155*, 3–10. [CrossRef]

5. Chalbaud, C.; Robin, M.; Lombard, J.M.; Martin, F.; Egermann, P.; Bertin, H. Interfacial tension measurements and wettability evaluation for geological CO_2 storage. *Adv. Water Resour.* **2009**, *32*, 98–109. [CrossRef]
6. Chalbaud, C.; Robin, M.; Bekri, S.; Egermann, P. Wettability Impact on CO_2 Storage in Aquifers: Visualisation and Quantification Using Micromodel Tests, Pore Network Model and Reservoir Simulations. In Proceedings of the International Symposium of the Society of Core Analysts, Calgary, AB, Canada, 10–12 September 2007; pp. 1–12.
7. Plug, W.J.; Bruining, J. Capillary pressure for the sand-CO_2-water system under various pressure conditions. Application to CO_2 sequestration. *Adv. Water Resour.* **2007**, *30*, 2339–2353. [CrossRef]
8. Lauren, S. Enhanced oil Recovery: How to Measure the Wettability of Carbonate Reservoir Core? *Biolin Sci. Surf. Sci. Blog* **2019**, 1–11. Available online: https://www.biolinscientific.com/blog/enhanced-oil-recovery-how-to-measure-the-wettability-of-carbonate-reservoir-core#:~:text=The-USBM-test-compares-the,spins-with-stepwise-increasing-speed (accessed on 3 March 2023).
9. Sagbana, P.I.; Sarkodie, K.; Nkrumah, W.A. A critical review of carbonate reservoir wettability modification during low salinity waterflooding. *Petroleum* **2022**, *9*, 317–330. [CrossRef]
10. Anderson, W.G. Wettability Literature Survey—Part 2: Wettability Measurement. *JPT J Pet. Technol.* **1986**, *38*, 1246–1262. [CrossRef]
11. Chaudhary, K.; Guiltinan, E.J.; Cardenas, M.B.; Maisano, J.A.; Ketcham, R.A.; Bennett, P.C. Wettability measurement under high P-T conditions using X-ray imaging with ap- plication to the brine-supercritical CO_2 system. *Geochem. Geophys. Geosystems* **2015**, *16*, 2858–2864. [CrossRef]
12. Kassa, A.M.; Gasda, S.E.; Landa-Marbán, D.; Sandve, T.H.; Kumar, K. Field-scale impacts of long-term wettability alteration in geological CO_2 storage. *Int. J. Greenh. Gas Control* **2022**, *114*, 103556. [CrossRef]
13. Kassa, A.M.; Gasda, S.E.; Kumar, K.; Radu, F.A. Impact of time-dependent wettability alteration on the dynamics of capillary pressure. *Adv. Water Resour.* **2020**, *142*, 103631. [CrossRef]
14. Zhu, L.; Liao, X.; Chen, Z.; Mu, L.; Wang, T. An analytical approach for evaluating the capillary trapping during CO_2 storage in aquifers. In *Society of Petroleum Engineers—SPE/IATMI Asia Pacific Oil and Gas Conference and Exhibition*; SPE: Lumpur, Malaysia, 2017; pp. 1–14.
15. Javanbakht, G.; Sedghi, M.; Welch, W.; Goual, L. Molecular dynamics simulations of CO_2/water/quartz interfacial properties: Impact of CO_2 dissolution in water. *Langmuir* **2015**, *31*, 5812–5819. [CrossRef] [PubMed]
16. Arif, M.; Abu-Khamsin, S.A.; Iglauer, S. Wettability of rock/CO_2/brine and rock/oil/CO_2-enriched-brine systems:Critical parametric analysis and future outlook. *Adv. Colloid Interface Sci.* **2019**, *268*, 91–113. [CrossRef] [PubMed]
17. Lv, P.; Liu, Y.; Wang, Z.; Liu, S.; Jiang, L.; Chen, J.; Song, Y. In Situ Local Contact Angle Measurement in a CO_2-Brine-Sand System Using Microfocused X-ray CT. *Langmuir* **2017**, *33*, 3358–3366. [CrossRef] [PubMed]
18. Al-yaseri, A.Z.; Lebedev, M.; Barifcani, A.; Iglauer, S. Receding and advancing (CO_2 + brine + quartz) contact angles as a function of pressure, temperature, surface roughness, salt type and salinity. *J. Chem. Thermodyn.* **2015**, *93*, 416–423. [CrossRef]
19. Sarmadivaleh, M.; Al-Yaseri, A.Z.; Iglauer, S. Influence of temperature and pressure on quartz-water-CO_2 contact angle and CO_2-water interfacial tension. *J. Colloid Interface Sci.* **2015**, *441*, 59–64. [CrossRef] [PubMed]
20. Alnili, F.; Al-Yaseri, A.; Roshan, H.; Rahman, T.; Verall, M.; Lebedev, M.; Sarmadivaleh, M.; Iglauer, S.; Barifcani, A. Carbon dioxide/brine wettability of porous sandstone versus solid quartz: An experimental and theoretical investigation. *J. Colloid Interface Sci.* **2018**, *524*, 188–194. [CrossRef]
21. Al-hadhrami, H.S.; Blunt, M.J. Thermally Induced Wettability Alteration to Improve Oil Recovery in Fractured Reservoirs. In Proceedings of the SPE/DOE Improved Oil Recovery Symposium, Tulsa, OK, USA, 22–26 April 2000; pp. 1–9.
22. Arif, M.; Al-Yaseri, A.Z.; Barifcani, A.; Lebedev, M.; Iglauer, S. Impact of pressure and temperature on CO_2-brine-mica contact angles and CO_2-brine interfacial tension: Implications for carbon geo-sequestration. *Colloid Interface Sci.* **2015**, *462*, 208–215. [CrossRef] [PubMed]
23. Botto, J.; Fuchs, S.J.; Fouke, B.W.; Clarens, A.F.; Freiburg, J.T.; Berger, P.M.; Werth, C.J. Effects of Mineral Surface Properties on Supercritical CO_2 Wettability in a Siliciclastic Reservoir. *Energy Fuels* **2017**, *31*, 5275–5285. [CrossRef]
24. Mutailipu, M.; Liu, Y.; Jiang, L.; Zhang, Y. Measurement and estimation of CO_2–brine interfacial tension and rock wettability under CO_2 sub- and super-critical conditions. *J. Colloid Interface Sci.* **2019**, *534*, 605–617. [CrossRef]
25. Jaeger, P.T.; Alotaibi, M.B.; Nasr-El-Din, H.A. Influence of compressed carbon dioxide on the capillarity of the gas-crude oil-reservoir water system. *J. Chem. Eng. Data* **2010**, *55*, 5246–5251. [CrossRef]
26. Saraji, S.; Piri, M.; Goual, L. The effects of SO_2 contamination, brine salinity, pressure, and temperature on dynamic contact angles and interfacial tension of supercritical CO_2/brine/quartz systems. *Int. J. Greenh. Gas Control* **2014**, *28*, 147–155. [CrossRef]
27. Liu, Y.; Mutailipu, M.; Jiang, L.; Zhao, J.; Song, Y.; Chen, L. Interfacial Tension and Contact Angle Measurements for the Evaluation of CO_2-Brine Two-Phase Flow Characteristics in Porous Media. *Environ. Prog. Sustain. Energy* **2015**, *34*, 1756–1762. [CrossRef]
28. Ameri, A.; Shojai Kaveh, N.; Rudolph, E.S.J.; Wolf, K.H.; Farajzadeh, R.; Bruining, J. Investigation on interfacial interactions among crude oil-brine-sandstone rock-CO_2 by contact angle measurements. *Energy Fuels* **2013**, *27*, 1015–1025. [CrossRef]
29. Drummond, C.; Israelachvili, J. Fundamental studies of crude oil-surface water interactions and its relationship to reservoir wettability. *J. Pet. Sci. Eng.* **2004**, *45*, 61–81. [CrossRef]
30. Chiquet, P.; Broseta, D.; Thibeau, S. Capillary Alteration of Shaly Caprocks by Carbon Dioxide. In Proceedings of the SPE Europec/EAGE Annual Conference, Madrid, Spain, 13–16 June 2005; pp. 1–10. [CrossRef]

31. Kaveh, N.S.; Rudolph, E.S.J.; Van Hemert, P.; Rossen, W.R.; Wolf, K.H. Wettability evaluation of a CO_2/water/bentheimer sandstone system: Contact angle, dissolution, and bubble size. *Energy Fuels* **2014**, *28*, 4002–4020. [CrossRef]
32. Wang, S.; Tao, Z.; Persily, S.M.; Clarens, A.F. CO_2 adhesion on hydrated mineral surfaces. *Environ. Sci. Technol.* **2013**, *47*, 11858–11865. [CrossRef]
33. Iglauer, S.; Pentland, C.H.; Busch, A. CO_2 wettability of seal and reservoir rocks and the implications for carbon geo-sequestration. *Water Resour. Res.* **2014**, *51*, 729–774. [CrossRef]
34. Daryasafar, A.; Keykhosravi, A.; Shahbazi, K. Modeling CO_2 wettability behavior at the interface of brine/CO_2/mineral: Application to CO_2 geo-sequestration. *J. Clean. Prod.* **2019**, *239*, 118101. [CrossRef]
35. Chiquet, P.; Broseta, D.; Thibeau, S. Wettability alteration of caprock minerals by carbon dioxide. *Geofluids* **2007**, *7*, 112–122. [CrossRef]
36. Bikkina, P.K. Contact angle measurements of CO_2-water-quartz/calcite systems in the perspective of carbon sequestration. *Int. J. Greenh. Gas Control* **2011**, *5*, 1259–1271. [CrossRef]
37. Mills, J.; Riazi, M.; Sohrabi, M. Wettability of common rock-forming minerals in a CO_2-brine system at reservoir conditions. In Proceedings of the International Symposium of the Society of Core Analysts, Austin, TX, USA, 21 August–1 September 2011; pp. 1–12.
38. Kim, Y.; Wan, J.; Kneafsey, T.J.; Tokunaga, T.K. Dewetting of Silica Surfaces upon Reactions with Supercritical CO_2 and Brine: Pore-Scale Studies in Micromodels. *Environ. Sci. Technol.* **2012**, *46*, 4228–4235. [CrossRef]
39. Hirasaki, G.J.; Miller, C.A.; Puerto, M. Recent Advances in Surfactant EOR. *SPE J.* **2011**, *16*, 889–907. [CrossRef]
40. Underschultz, J.; Boreham, C.; Dance, T.; Stalker, L.; Freifeld, B.; Kirste, D.; Ennis-King, J. CO_2 storage in a depleted gas field: An overview of the CO_2CRC Otway Project and initial results. *Int. J. Greenh. Gas Control* **2011**, *5*, 922–932. [CrossRef]
41. Zhang, X.; Ge, J.; Kamali, F.; Othman, F.; Wang, Y.; Le-Hussain, F. Wettability of sandstone rocks and their mineral components during CO_2 injection in aquifers: Implications for fines migration. *J. Nat. Gas Sci. Eng.* **2020**, *73*, 103050. [CrossRef]
42. Dai, Z.; Xu, L.; Xiao, T.; McPherson, B.; Zhang, X.; Zheng, L.; Dong, S.; Yang, Z.; Soltanian, M.R.; Yang, C.; et al. Reactive chemical transport simulations of geologic carbon sequestration: Methods and applications. *Earth-Sci. Rev.* **2020**, *208*, 103265. [CrossRef]
43. Juanes, R.; Spiteri, E.J.; Orr, F.M.; Blunt, M.J. Impact of relative permeability hysteresis on geological CO_2 storage. *Water Resour. Res.* **2006**, *42*, 1–13. [CrossRef]
44. Wang, S.; Liu, K.; Han, J.; Ling, K.; Wang, H.; Jia, B. Investigation of properties alternation during super-critical CO_2 injection in shale. *Appl. Sci.* **2019**, *9*, 1686. [CrossRef]
45. Li, Z.; Dong, M.; Li, S.; Huang, S. CO_2 sequestration in depleted oil and gas reservoirs-caprock characterization and storage capacity. *Energy Convers. Manag.* **2006**, *47*, 1372–1382. [CrossRef]
46. Li, S.; Dong, M.; Li, Z.; Huang, S.; Qing, H.; Nickel, E. Gas breakthrough pressure for hydrocarbon reservoir seal rocks: Implications for the security of long-term CO_2 storage in the Weyburn field. *Geofluids* **2005**, *5*, 326–334. [CrossRef]
47. Bachu, S. Sequestration of CO_2 in geological media: Criteria and approach for site selection in response to climate change. *Energy Convers. Manag.* **2000**, *41*, 953–970. [CrossRef]
48. Atkins, P.; de Paula, J. *Atkins' Physical Chemistry*, 8th ed.; Oxford University Press: Oxford, UK, 2006. [CrossRef]
49. Brendan, J. *Lowering Ethanol Carbon Intensity with CO_2 Capture and Enhanced Oil Recovery*; Great Plains Institute: Minneapolis, MN, USA, 2017.
50. Sampaio, M.A.; de Mello, S.F.; Schiozer, D.J. Impact of physical phenomena and cyclical reinjection in miscible CO_2-WAG recovery in carbonate reservoirs. *J. Pet. Explor. Prod. Technol.* **2020**, *10*, 3865–3881. [CrossRef]
51. Ampomah, W.; Balch, R.; Will, R.; Cather, M.; Gunda, D.; Dai, Z. Co-optimization of CO_2-EOR and Storage Processes under Geological Uncertainty. *Energy Procedia* **2017**, *114*, 6928–6941. [CrossRef]
52. Kashkooli, S.B.; Gandomkar, A.; Riazi, M.; Tavallali, M.S. Coupled optimization of carbon dioxide sequestration and CO_2 enhanced oil recovery. *J. Pet. Sci. Eng.* **2022**, *208*, 109257. [CrossRef]
53. Wang, X.; Jiang, L.; Gai, Z.; Tao, F.; Tang, H.; Xu, P. The plasticity of indigenous microbial community in a full-scale heavy oil-produced water treatment plant. *J. Hazard. Mater.* **2018**, *358*, 155–164. [CrossRef] [PubMed]
54. Chen, B.; Pawar, R.J. Capacity assessment and co-optimization of CO_2 storage and enhanced oil recovery in residual oil zones. *J. Pet. Sci. Eng.* **2019**, *182*, 106342. [CrossRef]
55. Azzolina, N.A.; Nakles, D.V.; Gorecki, C.D.; Peck, W.D.; Ayash, S.C.; Melzer, L.S.; Chatterjee, S. CO_2 storage associated with CO_2 enhanced oil recovery: A statistical analysis of historical operations. *Int. J. Greenh. Gas Control* **2015**, *37*, 384–397. [CrossRef]
56. Farajzadeh, R.; Eftekhari, A.A.; Dafnomilis, G.; Lake, L.W.; Bruining, J. On the sustainability of CO_2 storage through CO_2—Enhanced oil recovery. *Appl. Energy* **2020**, *261*, 114467. [CrossRef]
57. AlRassas, A.M.; Vo Thanh, H.; Ren, S.; Sun, R.; Al-Areeq, N.M.; Kolawole, O.; Hakimi, M.H. CO_2 Sequestration and Enhanced Oil Recovery via the Water Alternating Gas Scheme in a Mixed Transgressive Sandstone-Carbonate Reservoir: Case Study of a Large Middle East Oilfield. *Energy Fuels* **2022**, *36*, 10299–10314. [CrossRef]
58. Jia, K.; Zeng, J.; Wang, X.; Li, B.; Gao, X.; Wang, K. Wettability of Tight Sandstone Reservoir and Its Impacts on the Oil Migration and Accumulation: A Case Study of Shahejie Formation in Dongying Depression, Bohai Bay Basin. *Energies* **2022**, *15*, 4267. [CrossRef]
59. Khoshsima, A.; Sedighi, M.; Mohammadi, M. Enhanced oil recovery by water alternating gas injection. In *Gas Injection Methods: A Volume in Enhanced Oil Recovery Series*; Gulf Professional Publishing: Amsterdam, The Netherlands, 2023; pp. 295–316. [CrossRef]

60. Arzhilovsky, A.V.; Afonin, D.G.; Ruchkin, A.A.; Kobyashev, A.V.; Morozovskiy, N.A.; Toropov, K.V. Express assessment of the increase in the oil recovery as a result of water-alternating-gas technology application. *Neft. Khozyaystvo-Oil Ind.* **2022**, *2022*, 63–67. [CrossRef]
61. Lima, R.O.; de L. Cunha, A.; Santos, J.A.O.; Garcia, A.J.V.; dos Santos, J.P.L. Assessment of continuous and alternating CO_2 injection under Brazilian-pre-salt-like conditions. *J. Pet. Explor. Prod. Technol.* **2020**, *10*, 2947–2956. [CrossRef]
62. Nordic CCS Competence Centre Report. *The Nordic CO_2 Storage Atlas*; Nordic CCS Competence Centre Report: Copenhagen, Denmark, 2009.
63. Okamoto, I.; Li, X.; Ohsumi, T. Effect of supercritical CO_2 as the organic solvent on cap rock sealing performance for underground storage. *Energy* **2005**, *30*, 2344–2351. [CrossRef]
64. Sohrabi, M.; Fatemi, S.M.; Farzaneh, S.A.; Jami, M.; Ireland, S.; Ahmed, K. Performance of Swag Injection Versus Alternating and Continuous Injection of Water and Gas in Low Gas-Oil Ift and Mixed-Wet Systems. In Proceedings of the 26th International Symposium of the Society of Core Analysts, Aberdeen, UK, 27–30 August 2012; pp. 1–12.
65. Drozdov, A.; Gorbyleva, Y.; Drozdov, N.; Gorelkina, E. Perspectives of application of simultaneous water and gas injection for utilizing associated petroleum gas and enhancing oil recovery in the Arctic fields. *IOP Conf. Ser. Earth Environ. Sci.* **2021**, *678*, 012039. [CrossRef]
66. Heidari, P.; Kharrat, R.; Alizadeh, N.; Ghazanfari, M.H. A comparison of WAG and SWAG processes: Laboratory and simulation studies. *Energy Sources Part A Recover. Util. Environ. Eff.* **2013**, *35*, 2225–2232. [CrossRef]
67. Chen, P.; Sowaidi, A.K.A.; Patel, H.; Brantferger, K.; Bin Buang, K.A.; Syed, F.I.; Shehhi, R. Al Assessment of simultaneous water and gas injection swag pilot in a giant offshore carbonate reservoir. In Proceedings of the Abu Dhabi International Petroleum Exhibition & Conference, Abu Dhabi, United Arab Emirates, 7–10 November 2016; pp. 1–10. [CrossRef]
68. Shetty, S. *Evaluation of Simultaneous Water and Gas Injection Using CO_2*; Louisiana State University and Agricultural & Mechanical College: Baton Rouge, LA, USA, 2011.
69. Donaldson, E.C.; Chilingarin, G.V.; Yen, T.F. (Eds.) *Enhanced Oil Recovery, II process and operations*; Elsevier: Amsterdam, The Netherlands,, 1989; Volume 17B, pp. 1–607.
70. Teklu, T.W. *Experimental and Numerical Study of Carbon Dioxide Injection Enhanced Oil Recovery in Low-Permeability Reservoirs*; Colorado School of Mines: Golden, CO, USA, 2015; Volume 1.
71. Haeri, F.; Myshakin, E.M.; Sanguinito, S.; Moore, J.; Crandall, D.; Gorecki, C.D.; Goodman, A.L. Simulated CO_2 storage efficiency factors for saline formations of various lithologies and depositional environments using new experimental relative permeability data. *Int. J. Greenh. Gas Control* **2022**, *119*, 103720. [CrossRef]
72. Christensen, M.; Tanino, Y. Waterflood oil recovery from mixed-wet limestone: Dependence on contact anle. *Energy Fuels* **2015**, *31*, 1529–1535. [CrossRef]
73. dos Santos Lucas, C.R.; Aum, Y.K.P.G.; de Andrade Araújo, E.; de Castro Dantas, T.N.; Araújo, E.A.; Sousa, T.N.; Aum, P.T.P. Investigating the fluid-solid interaction of acid nonionic nanoemulsion with carbonate porous media. *Molecules* **2020**, *25*, 1475. [CrossRef]
74. Feldmann, F.; Al-Shalabi, E.W.; AlAmeri, W. Carbonate mineral effect on surface charge change during low-salinity imbibition. In *SPE Annual Technical Conference and Exhibition*; SPE: Lumpur, Malaysia, 2021; pp. 1–14. [CrossRef]
75. Zhou, L.; Liu, Y.; Anfinsen, B.; Hashemian, Y.; Yuan, Z. Evaluating Subsea Capping Stack Usage for CO_2 Blowouts Lei. In *Offshore Technology Conference*; OTC: Springfield, MO, USA, 2024; pp. 1–18. [CrossRef]
76. Wang, S.; Edwards, I.M.; Clarens, A.F. Wettability Phenomena at the CO_2–Brine–Mineral Interface: Implications for Geologic Carbon Sequestration. *Environ. Sci. Technol.* **2013**, *47*, 234–241. [CrossRef]
77. Eyitayo, S.I.; Arbad, N.; Kolawole, O.; Watson, M.C.; Eyitayo, S.I.; Arbad, N.; Kolawole, O.; Marshall, C. Optimizing CO_2 storage in deep saline formations: A comprehensive review of enhancing pore space utilization through simultaneous or alternate aquifer injection through simultaneous or alternate aquifer injection ABSTRACT. *Energy Sources Part A Recover. Util. Environ. Eff.* **2024**, *46*, 6513–6536. [CrossRef]
78. Dickson, J.L.; Gupta, G.; Horozov, T.S.; Binks, B.P.; Johnston, K.P. Wetting Phenomena at the CO_2/Water/Glass Interface. *Langmuir* **2006**, *22*, 2161–2170. [CrossRef]
79. Yang, D.; Gu, Y.; Tontiwachwuthikul, P. Wettability Determination of the Reservoir Brine−Reservoir Rock System with Dissolution of CO_2 at High Pressures and Elevated Temperatures. *Energy Fuels* **2007**, *22*, 504–509. [CrossRef]
80. Tonnet, N.; Broseta, D.F.; Mouronval, G. Evaluation of the Petrophysical Properties of a Carbonate-rich Caprock for CO_2 Geological Storage Purposes. In Proceedings of the 72nd European Association of Geoscientists and Engineers Conference and Exhibition 2010 A New Spring for Geoscience, Barcelona, Spain, 14–17 June 2010; Volume 2, pp. 802–814.
81. Espinoza, D.N.; Santamarina, J.C. Water-CO_2-mineral systems: Interfacial tension, contact angle, and diffusion—Implications to CO_2 geological storage. *Water Resour. Res.* **2010**, *46*. [CrossRef]
82. Broseta, D.; Tonnet, N.; Shah, V. Are rocks still water-wet in the presence of dense CO_2 or H2S? *Geofluids* **2012**, *12*, 280–294. [CrossRef]
83. Jung, J.-W.; Wan, J. Supercritical CO_2 and Ionic Strength Effects on Wettability of Silica Surfaces: Equilibrium Contact Angle Measurements. *Energy Fuels* **2012**, *26*, 6053–6059. [CrossRef]
84. Farokhpoor, R.; Bjørkvik, B.J.; Lindeberg, E.; Torsæter, O. CO_2 Wettability Behavior During CO_2 Sequestration in Saline Aquifer -An Experimental Study on Minerals Representing Sandstone and Carbonate. *Energy Procedia* **2013**, *37*, 5339–5351. [CrossRef]

85. Seyyedi, M.; Sohrabi, M.; Farzaneh, A. Investigation of Rock Wettability Alteration by Carbonated Water through Contact Angle Measurements. *Energy Fuels* **2015**, *29*, 5544–5553. [CrossRef]
86. Iglauer, S.; Mathew, M.; Bresme, F. Molecular dynamics computations of brine–CO_2 interfacial tensions and brine–CO_2–quartz contact angles and their effects on structural and residual trapping mechanisms in carbon geo-sequestration. *J. Colloid Interface Sci.* **2012**, *386*, 405–414. [CrossRef] [PubMed]
87. Tsuji, S.; Liang, Y.; Kunieda, M.; Takahashi, S.; Matsuoka, T. Molecular Dynamics Simulations of the CO_2-Water-silica Interfacial Systems. *Energy Procedia* **2013**, *37*, 5435–5442. [CrossRef]
88. Chen, C.; Dong, B.; Zhang, N.; Li, W.; Song, Y. Pressure and Temperature Dependence of Contact Angles for CO_2/Water/Silica Systems Predicted by Molecular Dynamics Simulations. *Energy Fuels* **2016**, *30*, 5027–5034. [CrossRef]
89. Yang, Y.; Nair, A.K.N.; Ruslan, M.F.A.C.; Sun, S. Interfacial properties of the alkane+water system in the presence of carbon dioxide and hydrophobic silica. *Fuel* **2021**, *310*, 122332. [CrossRef]
90. Zhu, Z.; Li, M.; Lin, M.; Peng, B.; Sun, L.; Chen, L. Investigation on Variations in Wettability of Reservoir Rock Induced by CO_2-Brine-rock Interactions. In Proceedings of the SPE EUROPEC/EAGE Annual Conference and Exhibition, Vienna, Austria, 23–26 May 2011; Volume 5, pp. 4027–4038.
91. Yang, D.; Gu, Y. Interfacial Interactions of Crude Oil-Brine-CO_2 Systems under Reservoir Conditions. SPE Annual Technical Conference and Exhibition. In Proceedings of the SPE Annual Technical Conference and Exhibition, Houston, TX, USA, 26–29 September 2004.
92. McCaughan, J.; Iglauer, S.; Bresme, F. Molecular Dynamics Simulation of Water/CO_2-quartz Interfacial Properties: Application to Subsurface Gas Injection. *Energy Procedia* **2013**, *37*, 5387–5402. [CrossRef]
93. Chen, C.; Chai, Z.; Shen, W.; Li, W.; Song, Y. Wettability of Supercritical CO_2–Brine–Mineral: The Effects of Ion Type and Salinity. *Energy Fuels* **2017**, *31*, 7317–7324. [CrossRef]
94. Al-Mutairi, S.M.; Abu-Khamsin, S.A.; Okasha, T.M.; Aramco, S.; Hossain, M.E. An experimental investigation of wettability alteration during CO_2 immiscible flooding. *J. Pet. Sci. Eng.* **2014**, *120*, 73–77. [CrossRef]
95. Ali, M.; Arif, M.; Sahito, M.F.; Al-Anssari, S.; Keshavarz, A.; Barifcani, A.; Stalker, L.; Sarmadivaleh, M.; Iglauer, S. CO_2-wettability of sandstones exposed to traces of organic acids: Implications for CO_2 geo-storage. *Int. J. Greenh. Gas Control* **2019**, *83*, 61–68. [CrossRef]
96. da Costa, A.A.; Costa, G.; Embiruçu, M.; Soares, J.B.; Trivedi, J.J.; Rocha, P.S.; Souza, A.; Jaeger, P. The Influence of Rock Composition and pH on Reservoir Wettability for Low-Salinity Water-CO_2 Enhanced Oil Recovery Applications in Brazilian Reservoirs. *SPE Reserv. Evaluation Eng.* **2020**, *24*, 45–65. [CrossRef]
97. Ali, M.; Awan, F.U.R.; Ali, M.; Al-Yaseri, A.; Arif, M.; Sánchez-Román, M.; Keshavarz, A.; Iglauer, S. Effect of humic acid on CO_2-wettability in sandstone formation. *J. Colloid Interface Sci.* **2020**, *588*, 315–325. [CrossRef]
98. Ali, M.; Al-Yaseri, A.; Awan, F.U.R.; Arif, M.; Keshavarz, A.; Iglauer, S. Effect of water-soluble organic acids on wettability of sandstone formations using streaming zeta potential and NMR techniques: Implications for CO_2 geo-sequestration. *Fuel* **2022**, *329*. [CrossRef]
99. Liu, S.; Yang, X.; Qin, Y. Molecular dynamics simulation of wetting behavior at CO_2/water/solid interfaces. *Chin. Sci. Bull.* **2010**, *55*, 2252–2257. [CrossRef]

Disclaimer/Publisher's Note: The statements, opinions and data contained in all publications are solely those of the individual author(s) and contributor(s) and not of MDPI and/or the editor(s). MDPI and/or the editor(s) disclaim responsibility for any injury to people or property resulting from any ideas, methods, instructions or products referred to in the content.